REPORT DOCUMENTATION PAGE

Form Approved
OMB No. 0704-0188

1. REPORT DATE *(DD-MM-YYYY)*	**2. REPORT TYPE**	**3. DATES COVERED** *(From - To)*
January 2014	Journal Article	January 2014- March 2014

4. TITLE AND SUBTITLE
Silicon-Containing Tri- and Tetra-Functional Cyanate Esters: Synthesis, Cure Kinetics, and Network Properties

5a. CONTRACT NUMBER
In-House

5b. GRANT NUMBER

5c. PROGRAM ELEMENT NUMBER

6. AUTHOR(S)
Andrew J Guenthner , Vandana Vij, Timothy S. Haddad, Josiah T. Reams, Kevin R. Lamison, Christopher M. Sahagun, Sean M. Ramirez Gregory R Yandek, Suresh C Suri Joseph M Mabry

5d. PROJECT NUMBER

5e. TASK NUMBER

5f. WORK UNIT NUMBER
Q0BG

7. PERFORMING ORGANIZATION NAME(S) AND ADDRESS(ES)

Air Force Research Laboratory (AFMC)
AFRL/RQRP
10 E. Saturn Blvd.
Edwards AFB CA 93524-7680

8. PERFORMING ORGANIZATION REPORT NO.

9. SPONSORING / MONITORING AGENCY NAME(S) AND ADDRESS(ES)
Air Force Research Laboratory (AFMC)
AFRL/RQR
5 Pollux Drive
Edwards AFB CA 93524-7048

10. SPONSOR/MONITOR'S ACRONYM(S)

11. SPONSOR/MONITOR'S REPORT NUMBER(S)
AFRL-RQ-ED-JA-2013-249

12. DISTRIBUTION / AVAILABILITY STATEMENT
Distribution A: Approved for Public Release; Distribution Unlimited. PA#13541

13. SUPPLEMENTARY NOTES
Journal Article submitted to Journal of Polymer Science Part A: Polymer Chemistry.

14. ABSTRACT
The synthesis and physical properties of new silicon-containing polyfunctional cyanate ester monomers tris(4-cyanatophenyl)methylsilane and tetrakis(4-cyanatophenyl)silane, as well as polycyanurate networks formed from these monomers are reported. The higher cross-linking functionality compared to di(cyanate ester) monomers enables much higher ultimate glass transition temperatures to be obtained as a result of thermal cyclotrimerization. The ability to reach complete conversion is greatly enhanced by cocure of the new monomers with di(cyanate ester) monomers such as 1,1-bis(4-cyanatophenyl)ethane (LECy). The presence of silicon in these polycyanurate networks imparts improved thermochemical stability in air compared to carbon-containing analogs in cases where the thermochemical performance in air is significantly worse than under nitrogen. The water uptake in the silicon-containing networks examined is 4 – 6 wt% after 96 hours of immersion at 85 °C, considerably higher than both carbon-containing and/or di(cyanate ester) analogs.

15. SUBJECT TERMS

16. SECURITY CLASSIFICATION OF:			**17. LIMITATION OF ABSTRACT**	**18. NUMBER OF PAGES**	**19a. NAME OF RESPONSIBLE PERSON**
					Joseph Mabry
a. REPORT	**b. ABSTRACT**	**c. THIS PAGE**	SAR	58	**19b. TELEPHONE NO** *(include area code)*
Unclassified	**Unclassified**	**Unclassified**			661-525-5857

Standard Form 298 (Rev. 8-98)
Prescribed by ANSI Std. 239.18

Silicon-Containing Tri- and Tetra-Functional Cyanate Esters: Synthesis, Cure Kinetics, and Network Properties

Andrew J. Guenthner,[1] Vandana Vij,[2] Timothy S. Haddad,[2] Josiah T. Reams,[2] Kevin R. Lamison,[2] Christopher M. Sahagun,[3] Sean M. Ramirez,[2] Gregory R. Yandek,[1] Suresh C. Suri,[1] and Joseph M. Mabry[1]

[1] Aerospace Systems Directorate, Air Force Research Laboratory, Edwards AFB, CA 93524

[2] ERC Incorporated, Air Force Research Laboratory, Edwards AFB, CA 93524

[3] National Research Council / Air Force Research Laboratory, Edwards AFB, CA 93524

Correspondence to: Andrew J. Guenthner (E-mail: *andrew.guenthner@edwards.af.mil*)

Additional Supporting Information may be found in the online version of this article.

ABSTRACT

The synthesis and physical properties of new silicon-containing polyfunctional cyanate ester monomers tris(4-cyanatophenyl)methylsilane and tetrakis(4-cyanatophenyl)silane, as well as polycyanurate networks formed from these monomers are reported. The higher cross-linking functionality compared to di(cyanate ester) monomers enables much higher ultimate glass transition temperatures to be obtained as a result of thermal cyclotrimerization. The ability to reach complete conversion is greatly enhanced by cocure of the new monomers with di(cyanate ester) monomers such as 1,1-bis(4-cyanatophenyl)ethane (LECy). The presence of silicon in these polycyanurate networks imparts improved thermochemical stability in air compared to carbon-containing analogs in cases where the thermochemical performance in air is significantly worse than under nitrogen. The water uptake in the silicon-containing networks examined is 4 – 6 wt% after 96 hours of immersion at 85 °C, considerably higher than both carbon-containing and/or di(cyanate ester) analogs.

KEYWORDS cyanate ester, silane, polycyanurate, thermoset, differential scanning calorimetry

INTRODUCTION

Polycyanurate networks formed from the cyclotrimerization of cyanate ester monomers have proven to be an especially useful class of thermosetting material, with numerous high-performance applications in the micro-electronics and aerospace industries.[1-4] Some of the more interesting example applications include magnet casing for nuclear fusion reactors[5,6] and the Large Hadron Collider,[7] brush seals for turbine engines,[8,9] and spacecraft structures such as frameworks for telescope mirrors[10] and solar panel supports.[11] In many applications, protection against oxidation during short-term exposure to temperatures at or above 500 °C is highly desirable. Unfortunately, the onset of thermochemical

degradation in the triazine cross-links of cyanurate networks occurs well below 500 °C,[12] thus thermo-oxidative protection must be provided by the incorporation of more stable materials.

A strategy for providing thermo-oxidative protection to cyanurate polymer networks that has been explored through much recent investigation is the incorporation of silicon or siloxy moieties in the form of monomers and co-curatives,[13-21] blends and modifiers,[22-24] silica nanoparticles,[25-38] clay nanoplatelets,[39-53] or other silicon-containing nanostructures[54-60] including oligomeric silsesquioxanes.[61-75] While the addition of fully oxidized silica (type "Q" silicates) can provide an in-place barrier to oxygen permeation, the use of unoxidized organosilicon moieties or partly oxidized silicates (type "M", "D", or "T"), allows for the *in-situ* generation of a protective barrier during high-temperature oxidation or exposure to energetic forms of oxygen (such as atomic oxygen in low Earth orbit).[76-78] Such *in-situ* generation from the bulk has the advantage of spontaneous re-generation in the event that a protective layer is breached or damaged during exposure. Furthermore, the incorporation of silicon at the molecular level by the use of organosilicon small-molecule monomers (either as single component substitutes or cocuratives) can preserve desirable processing characteristics such as a low viscosity in the uncured state.

To date, there have been several reports relating to organosilicon monomers for epoxy,[13,14,79-83] benzoxazine,[84] and bismaleimide[18,85-87] thermosetting networks. In cyanate esters, a silicon-containing analog (named SiMCy) to the well-known dicyanate ester of bisphenol A (BADCy) was first synthesized by Wright et al. in 2003.[20] Compared to BADCy, SiMCy exhibited improved thermo-oxidative resistance at high temperatures along with lower water uptake, and improved processing and cure characteristics.[19] Two cyanate ester organosilane monomers have also been described recently for use in the formation of microporous structures.[15]

Though the incorporation of silicon at the molecular level in thermosetting polymers offers improved thermo-oxidative resistance, it can have negative effects on other aspects of performance. Because the carbon-silicon bond is in general longer and more flexible than a corresponding carbon-

carbon bond, the molecular segments of networks containing such bonds are more flexible, resulting in a lower glass transition temperature at full cure, when silicon is incorporated into the network. Approaches to the molecular-level incorporation of silicon that enable the networks to retain high glass transition temperatures at full cure are therefore of considerable interest. To date, however, there has been very little work devoted to demonstrating means of incorporating molecular-level silicon in a manner that facilitates the retention of high glass transition temperatures at full cure.

In this paper, we report on the synthesis, cure kinetics, and network properties of tri- and tetra-functional silicon-containing cyanate esters in which the silicon serves as a network junction point after cure. It has been shown that the incorporation of network junctions, whether they arise from cross-links or from branch points in tri- (or higher) functional monomers with functional end groups, provide for an increased glass transition temperature at full cure in thermosetting composite resins.[88] By incorporating silicon into tri- and tetra-functional monomers in such a way as to create a network junction coincident with each incorporated silicon atom, we show that networks are obtained that exhibit glass transition temperatures higher than those of the corresponding networks formed from di-functional cyanate esters without silicon. We further show that these advantages are retained when the silicon-containing monomers are cocured with di(cyanate esters) such as Primaset® LECy in order to achieve complete conversion to cyanurate. These networks thus offer both high glass transition temperatures as well as increased thermo-oxidative stability while retaining good processing characteristics.

EXPERIMENTAL

General Considerations. All manipulations of compounds and solvents were carried out using standard Schlenk line techniques. Tetrahydrofuran (THF), ether, chloroform, hexane and toluene were dried by passage through columns of activated alumina under a nitrogen atmosphere and then degassed prior to use. Dichloromethane and acetone solvents were purchased as the anhydrous grade from Aldrich and used as received. Trichloromethylsilane and tetrachlorosilane were purchased from

Gelest and were distilled before use. Triethylamine was purchased from Aldrich Chemical Co and distilled before use. 4-Benzyloxybromobenzene was obtained from Aldrich and recrystallized from ether before use. Cyanogen bromide, n-butyllithium, nonylphenol, and 10% palladium on carbon (wet, Degussa type) were obtained from Aldrich Chemical Co. and used as received. Copper(II) acetylacetonate was purchased from Ric/Roc and used as received. ^{1}H, ^{13}C and ^{29}Si NMR measurements were performed using a Bruker AC 300 or Bruker 400 MHz instrument. ^{1}H and ^{13}C NMR chemical shifts are reported relative to the deuterated solvent peak (^{1}H, ^{13}C: acetone-d6, δ 2.05 ppm, δ 29.9 ppm or $CDCl_3$, δ 7.28 ppm, δ 77.23 ppm). ^{29}Si NMR chemical shifts are reported relative to external tetramethylsilane at 0 ppm. Hydrogenation was done using a Parr Hydrogenator equipped with pressure safe vessels and Viton® seals. Selected cyanate ester samples were purified using a W-Prep2XY Yamazen chromatographic column. For characterization, samples were run on a TA Instruments Q2000 Differential Scanning Calorimeter (DSC) under nitrogen flowing at 50 mL/ min, with 5 minutes for equilibration at the maximum and minimum temperatures, to establish the melting point from a consistent thermal condition. Elemental analyses were obtained from Atlantic Microlabs or performed on a Perkin Elmer EA2400 Series II combustion analyzer.

Preparation of tris (4-benzyloxyphenyl)methylsilane (1). A chilled (-78 °C) THF (400 mL) solution of 4-bromophenyl benzyl ether (20.00 g, 76.0 mmol was treated with 2.5M n-BuLi (30.4 mL, 76 mmol) and allowed to react with stirring for 2 h at -78 °C. This mixture, now heterogeneous, was treated with slow addition of trichloromethylsilane (3.787 g, 25.33 mmol, diluted with THF) and the cooling bath removed. The mixture was allowed to react with stirring overnight, then the solvents were removed under reduced pressure. Chloroform (300 mL) was added and the mixture was stirred for additional hour. This was filtered to remove LiCl salt and the solvent from the filtrate was removed under reduced pressure on a rotary evaporator. The off-white crude product was precipitated into methanol (400 mL). This was stirred overnight, filtered and dried under nitrogen to afford **1** as a white solid (13 g, 87% yield). ^{1}H NMR (acetone-d6) δ: 7.48 to 7.32 (m, 21H), 7.03 (d, J = 8 Hz, 6H), 5.12 (s, 6H), 0.75 (s, 3H). ^{13}C NMR

(acetone-d6) δ: 160.94 (C4), 138.32 (C6), 137.47 (C2), 136.86 (C1), 129.35 (C8), 128.70 (C9), 128.50 (C7), 115.38 (C3), 70.23 (C5), -2.66 (C10, $SiCH_3$). ^{29}Si NMR (acetone-d6) δ: -12.32 (s). Combustion analysis Calculated (Found): % C, 81.04 (80.77); % H, 6.12 (6.13).

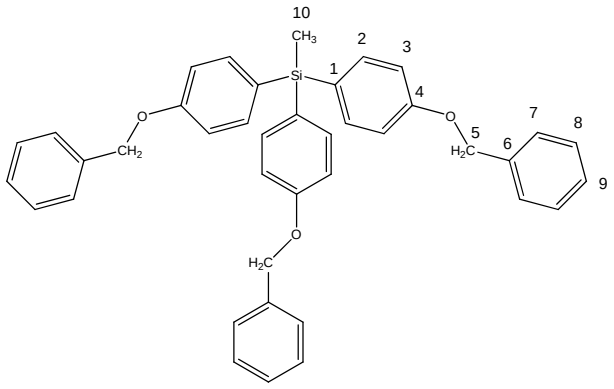

Preparation of tris (4-hydroxyphenyl) methylsilane (2). A THF (200 mL) solution containing **1** (10.00 g, 16.89 mmol) and 10 wt % palladium on carbon (400 mg), was placed in a 1000 mL pressure safe vessel equipped with Viton® seals and connected to a hydrogenator. This was pressurized with hydrogen (35 psi) and allowed to react with stirring for 48 hr. The catalyst was removed by filtration through Celite, and the solvent was removed under reduced pressure to afford 4.60 g (85 % yield) of **2**, as an off-white solid. For purification, compound **2** was dissolved in THF and precipitated out in hexane. The white product was filtered, washed with ether and dried under dynamic vacuum. ^{1}H NMR (acetone-d6) δ: 8.47 (s, 3H), 7.34 (d, J = 8 Hz, 6H), 6.87 (d, J = 8 Hz, 6H), 0.70 (s, 3H). ^{13}C NMR (acetone-d6) δ: 159.43 (C4), 137.52 (C2), 127.37 (C1), 115.92 (C3), -2.51 (C5, $SiCH_3$). ^{29}Si NMR (acetone-d6) δ: -12.57 (s). Combustion analysis Calculated (Found): % C, 70.78 (70.35); % H, 5.63 (5.69).

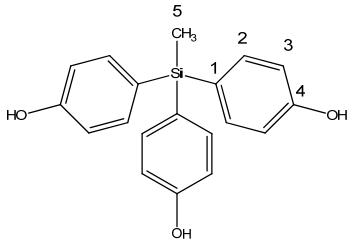

Preparation of tris(4-cyanatophenyl) methylsilane (3). A chilled (-20 °C) ether (200 mL) solution containing tris(4-hydroxyphenyl) methylsilane, **2**, (4.0 g, 12.41 mmol) and cyanogen bromide (4.88 g, 46.53 mmol) was treated with triethylamine (4.71 g, 46.53 mmol) in a drop-wise manner. This mixture was allowed to react for 2 hr with stirring at -20 °C. Diethyl ether (500 mL) was added to the reaction mixture and stirred overnight. The mixture was filtered to remove the hydrobromide salt, and the organic layer was washed with (2 X 100 mL) DI water, followed by a brine wash and then dried over $MgSO_4$. The solvents were removed under reduced pressure, and crude product (3.2 g, 80 % yield) was precipitated out from ether to afford 2.9 g (72 % yield) of **3** as white crystalline solid (mp 118 °C). Some batches of cyanate ester **3** were further purified by flash chromatography using silica-gel (40μm, 60 Å) universal column size M (20 ID x 80 mm packed length) under gradient condition. ^{1}H NMR (acetone-d6) δ: 7.74 (d, J = 9 Hz, 6H), 7.48 (d, J = 9 Hz, 6H), 0.98 (s, 3H). ^{13}C NMR (acetone-d6) δ: 154.48(C4), 137.37 (C2), 134.11 (C1), 115.13 (C3), 108.20 (C6, OCN), -4.43 (C5, $SiCH_3$). ^{29}Si NMR (acetone-d6) δ: -10.51 (s). Combustion analysis Calculated (Found): % C, 66.48 (66.01); % H, 3.80 (3.68); % N, 10.57 (10.68).

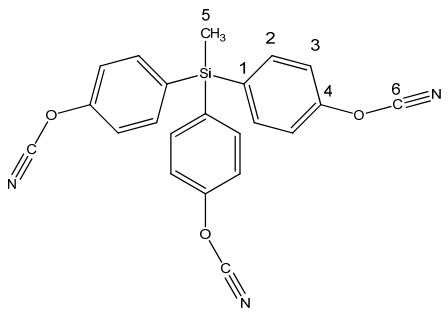

Preparation of tetrakis (4-benzyloxyphenyl) silane (4). A chilled (-78 °C) THF (400 mL) solution of 4-bromophenyl benzyl ether (20.00 g, 76.0 mmol was treated with 2.5M n-BuLi (30.4 mL, 76 mmol) and allowed to react with stirring for 2 h at -78 °C. This mixture, now heterogeneous, was treated with a slow addition of tetrachlorolsilane (3.22 g, 19 mmol, diluted with THF) and the cooling bath removed. The mixture was allowed to reflux at 55^0 C with stirring for two nights. The solvents were removed under reduced pressure. Chloroform (300 mL) was added and the mixture was stirred for additional hour. This was filtered to remove LiCl salt and the solvent from the filtrate was removed under reduced pressure on a rotary evaporator. The off-white crude product was precipitated into methanol (400 mL). This was stirred overnight, filtered and dried under nitrogen to afford **4** as a white solid (11 g, 76% yield). ^{1}H NMR ($CDCl_3$) δ: 7.54 -7.38 (m, 28H), 7.05 (d, J = 9 Hz, 8H), 5.12 (s, 8H). ^{13}C NMR ($CDCl_3$) δ: 160.54 (C4), 137.84 (C2), 136.98 (C6), 128.66 (C8), 128.06 (C9), 127.59 (C7), 126.42 (C1), 114.46 (C3), 69.80 (C5). ^{29}Si NMR ($CDCl_3$) δ: -14.60 (s). Combustion analysis Calculated (Found): % C, 82.07 (81.49); % H, 5.83 (5.90).

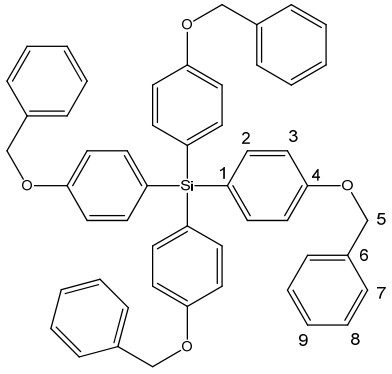

Preparation of tetrakis(4-hydroxyphenyl) silane (5). A THF (200 mL) solution containing **4** (10.00 g, 13.15 mmol) and 10 wt % palladium on carbon (400 mg) was placed in a 1000 mL pressure safe vessel equipped with Viton® seals and connected to a hydrogenator. This was placed under an atmosphere of hydrogen (35 psi) and allowed to react with stirring for 48 hr. The catalyst was removed by filtration through Celite, and the solvent was removed under reduced pressure to afford 4.80 g (91 % yield) of **5** as

an off-white solid. For purification, compound **5** was dissolved in THF and precipitated out in hexane. The white product was filtered, washed with ether and dried under dynamic vacuum. ^{1}H NMR (acetone-d6) δ: 8.63 (s, 4H), 7.38 (d, J = 6 Hz, 8H), 6.81 (d, J = 6 Hz, 8H). ^{13}C NMR (acetone-d6) δ: 159.54 (C4), 138.59 (C2), 125.98 (C1), 115.92 (C3). ^{29}Si NMR (acetone-d6) δ: -14.64 (s). Combustion analysis Calculated (Found): % C, 71.97 (68.89); % H, 5.03 (5.55).

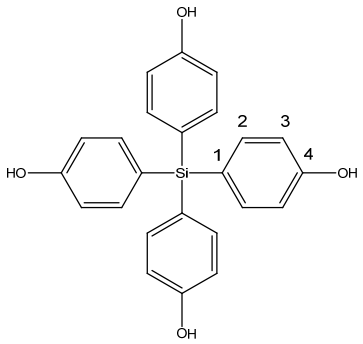

Preparation of tetrakis(4-cyanatophenyl) silane (6). A chilled (-20 °C) ether (200 mL) and THF (5 mL) solution containing tetrakis(4-hydroxyphenyl) silane, **5**, (4.0 g, 10 mmol) and cyanogen bromide (5.22 g, 50.mmol) was treated with triethylamine (5.06 g, 50 mmol) in a drop-wise manner. This mixture was allowed to react for 2 hr with stirring at -20 °C. Dichloromethane (200 mL) was added to the reaction mixture and stirred for an hour. The mixture was filtered to remove the hydrobromide salt, and the organic layer was washed with (2 X 100 mL) DI water, followed by a brine wash and then dried over $MgSO_4$. The solvents were removed under reduced pressure, and crude product (3.8 g, 76 % yield) was precipitated from ether to afford 3.5 g (72 % yield) of **6** as white crystalline solid (mp 169 °C). ^{1}H NMR (acetone-d6) δ: 7.77 (d, J = 8, 8H), 7.54 (d, J = 8, 8H). ^{13}C NMR (acetone-d6) δ: 155.73 (C4), 139.72 (C2), 132.38 (C1), 116.40 (C3), 109.02 (C5, OCN). ^{29}Si NMR (acetone-d6) δ: -14.95 (s). Combustion analysis Calculated (Found): % C, 67.19 (67.21); % H, 3.22 (3.27); % N, 11.19 (10.84).

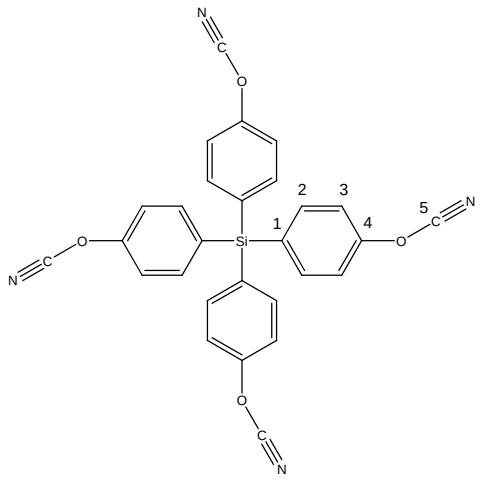

Preparation of thermally cured networks. Cured networks were prepared from the newly synthesized cyanate esters (**3**) and (**6**), blends of (**3**) and (**6**) with the commercial dicyanate ester Primaset® LECy (1,1-bis(4-cyanatophenol)ethane, purchased from Lonza and used as received), and three different "control" materials: 1) Primaset® BADCy (2,2-bis(4-cyanatophenyl)propane), purchased from Lonza and used as received), 2) SiMCy (bis(4-cyanatophenyl)dimethylsilane), prepared according to a previously published procedure),[17] and 3) ESR-255[89] (1,1,1-tris(4-cyanatophenyl)ethane), also prepared according to a previously published procedure by Dr. Mathew Davis of NAWCWD.[90] The properties of SiMCy[16,17,19,20] and ESR-255[89,90] have been described in numerous previous publications. To assess the effects of purity, some batches of (**3**) and SiMCy were purified by passing solutions in dichloromethane through a W-Prep2XY Yamazen flash chromatograph, followed by precipitation into methanol.

Figure 1 provides the structures of all the networks synthesized. ESR-255 is the carbon-containing analog of the silicon-containing tricyanate (3). SiMCy is the dicyanate analog of (3) in which one cyanate ester functional arm has been replaced by a methyl group, and BADCy is the carbon-containing analog of SiMCy. The carbon-containing analog of (6) has been reported previously,[91] but was difficult to cure into a network, thus little physical property data is available. Previous work on tricyanate esters has shown that preparing networks comprising 50 wt% of the dicyanate with 50 wt% LECy can result in synergistic improvements in performance.[92] Thus, networks were also prepared from

mixtures of equal parts by weight of (**3**) with LECy and (**6**) with LECy, as well as with equal parts of ESR-255 and LECy for comparison. For all investigations, no catalysts were added to the monomers prior to network formation.

To mix monomers for cocuring of blended networks, equal weights of each component were weighed out into a vial and then heated to 10 – 20 °C above the highest melting point of any of the system components and stirred together. An analogous procedure was used for single-component networks except that no stirring was required. Once prepared in a homogeneous, molten state, networks were de-gassed for 30 minutes under reduced pressure (approximately 300 mm Hg), then poured into cylindrical molds measuring 12 mm in diameter x about 3 mm deep composed of silicone rubber. Details of the mold-making procedure have been published elsewhere.[93] The samples were then heated under dry nitrogen to 150 °C for 1 hour, followed by 210 °C for 24 hours, using ramp rates of 5 °C / min. Once cooled, the samples were de-molded to form homogeneous discs.

Characterization. Differential scanning calorimetry (DSC) was carried out on a TA Instruments Q Series 200 instrument under 50 mL/min. dry nitrogen purge. Several different programs were used for analysis. Standard non-isothermal analysis involved heating samples at 10 °C / min to 350 °C, cooling at 10 °C / min. to 100 °C, then re-heating to 350 °C at 10 °C / min to establish a baseline. For cure kinetics studies, samples were first heated at 5 °C / min. to 130 °C to achieve any required melting, then heated as fast as possible (~100 °C/min.) to the desired isothermal cure temperature and held for 30 minutes isothermally. Following the isothermal cure, the samples were quenched (~100 °C/min. cooling) to 120 °C, then heated to 350 °C at 10 °C / min. The samples were then cooled at 10 °C / min. to 100 °C, and the entire procedure was repeated with the cured sample in place to establish a baseline. The details of this procedure, including the method of applying baseline corrections, have been published previously.[90] Cure kinetics were determined using the Kamal model[94] with a variant of Kenny's graphical method;[95] complete details of this procedure have also been published previously.[90]

Thermogravimetric analysis (TGA) was carried out using a TA Instruments Q5000 under 50 mL/min. sample gas purge (dry nitrogen or air), and 10 mL/min. balance gas purge (with gas type matched to the sample). TGA samples were comprised of small chunks of cured discs, and were heated at 10 °C/min. to 600 °C. Oscillatory thermomechanical analysis (TMA) was performed using a TA Instruments Q400, with a 50 mL/min. dry nitrogen purge. Cured discs were subjected to a mean compressive force of 0.1 N, oscillating with an amplitude of 0.1 N and a frequency of 0.05 Hz. Samples were pre-loaded with a 0.2 N force to help achieve good contact with the probe, which consisted of the 5 mm diameter cylindrical "standard" quartz probe supplied by TA Instruments. For "dry" TMA analysis, samples were cycled between 100 °C and 200 °C twice at 10 °C / min. to measure thermal lag (details of this procedure are published elsewhere),[93] then heated to 350 °C at 10 °C / min., cooled to 100 °C at 10 °C / min., then re-heated to 350 °C at 10 °C / min. For "wet" TMA analysis, samples were first heated to 350 °C, then cycled between 100 °C and 200 °C to measure thermal lag, then re-heated to 350 °C, all at 20 °C / min. The procedure for "wet" TMA is designed to minimize drying of the sample prior to measurement of the glass transition temperature.

Crystal data for compounds (**3**) and (**6**) was collected at T=100.0 (K) using Kusing Bruker 3-circle, SMARTAPEX CCD with c-axis fixed at 54.748, running on SMART V 5.625 program (Bruker AXS: Madison, 2001). Graphite monochromated $Mo_{K\alpha}$ (λ= 0.71073 Å) radiation was employed for data collection and corrected for Lorentz and polarization effects using SAINT V 6.22 program (Bruker AXS: Madison, 2001), and reflection scaling (SADABS program, Bruker AXS: Madison, WI, 2001). Structures were solved by direct methods (SHELXL-97, Bruker AXS: Madison, 2000) and all non-hydrogen atoms refined anisotropically using full-matrix least-squares refinement on F^2. Hydrogen atoms were added at calculated positions when necessary. CDCC 960730 (SiCy-3) and CDCC 960731 (SiCy-4) contains the supplementary crystallographic data for this paper. This data can be obtained free of charge from the Cambridge Crystallographic Data Centre via www.ccdc.cam.ac.uk/data_request/cif.

Densities were determined by immersing cured discs in solutions of $CaC1_2$ and varying the $CaCl_2$ concentration until neutral buoyancy was achieved. The density of the fluid needed to achieve neutral buoyancy was then determined by weighing 10.00 mL of the fluid in a volumetric flask.

RESULTS AND DISCUSSION

Synthesis of New Monomers (3) and (6).

The new cyanate ester monomers (**3**) and (**6**) were synthesized following the procedures similar to those published for production of SiMCy[17] (See Scheme 1). Lithium-bromo exchange on *p*-bromophenyl benzyl ether with butyllithium produces a nucleophile which can be used to replace all the chlorides on tetrachlorosilane or methyltrichlorosilane with benzyloxyphenyl groups to produce compounds (**1**) and (**4**). The "protecting" benzyl group is easily removed by low-pressure hydrogenation catalyzed with 10% palladium on carbon to produce the phenols (**2**) and (**5**). These phenols react in high yield with cyanogen bromide in the presence of triethylamine to make the desired cyanate ester monomers (**3**) and (**6**). All six compounds were isolated in high yield and fully characterized by combustion analysis and ^{1}H, ^{13}C and ^{29}Si NMR spectroscopy. Their spectra are simple and unremarkable with chemical shifts all in the expected regions and ratios. This data is presented in the experimental section. Additional verification of the structure of (**3**) and (**6**) was provided by X-Ray Diffraction of single crystals. The resultant structures are shown in Figures 2 and 3. All bond angles and bond lengths are in the expected ranges for such compounds.

Cure Characteristics of Monomers (3) and (6).

The non-isothermal DSC scan shown in Figure 4 for SiCy-3 (**3**) after purification by chromatography is typical for highly pure cyanate ester monomers, with re-crystallization of the

supercooled melt at 50-100 °C followed by melting at 118 °C, a very wide processing window, and cyclotrimerization onset near 300 °C. Both the melting temperature and enthalpy are very similar to that of 1,1,1-tris(4-cyanatophenyl)ethane (known as ESR-255), the carbon-containing analog of SiCy-3. (A full set of comparative non-isothermal DSC data for all monomers studied is provided in Supporting Information Section S2.) The "L"-shaped exotherm associated with cure is indicative of incomplete conversion, as further indicated by an enthalpy of cyclotrimerization of 94 ± 4 kJ per cyanate equivalent, *versus* an expected value of around 110 kJ/eq. In fact the enthalpies of cyclotrimerization for SiCy-3 and ESR-255 are not significantly different when measured by the same non-isothermal DSC protocol, indicating that the more flexible C-Si linkages are ineffective at relieving the steric constraints that prevent complete cyclotrimerization of these tricyanate monomers. From the perspective of vitrification, the incomplete conversion after heating to 350 °C, coupled with the absence of any detectable glass transition temperature in samples heated to 350 °C, strongly indicates that networks from SiCy-3 and its tetracyanate ester analog are able to achieve glass transition temperatures well in excess of 350 °C if sufficiently cyclotrimerized, and that their maximum attainable use temperatures are, like ESR-255, limited by thermal decomposition rather than softening if sufficient cyclotrimerization is achieved.

The non-isothermal DSC of SiCy-4 (Figure 5) indicates that similar steric constraints on cyclotrimerization exist for the tetracyanate analog of SiCy-3. Furthermore, the high melting point precludes many low-cost processing operations. Due to its low potential for use further work with the neat monomer, including purification by chromatography, was not attempted, although promising results were obtained when cocured with Primaset® LECy (*vide infra*). As a result of the lower purity, the cyclotrimerization exotherm is shifted to much lower temperatures, resulting in a very prominent "L"-shaped exotherm. The total enthalpy of cyclotrimerization (at 96 ± 10 kJ/eq.), is not significantly different from SiCy-3.

Isothermal DSC analysis of the cyclotrimerization of SiCy-3 produced a pattern of conversion as a function of time and temperature similar to most cyanate ester monomers, as seen in Figure 6. The cure kinetics up to 50% conversion were described well by the Kamal model[94] using analysis procedures that have been described in detail elsewhere.[90] (A complete listing of model parameter values and conversion as a function of time and temperature graphs for SiCy-3 and its many analogs, including analysis of batch to batch reproducibility and effects of purity level, are provided in Supporting Information Section S3). Arrhenius analysis of the cyclotrimerization of SiCy-3 after purification by chromatography (Figure 7) resulted in an estimated activation energy of 115 ± 1 kJ/mol. Note that this uncertainty estimate reflects only the precision of the Arrhenius model fit to the data. When two separate batches of SiCy-3 were analyzed, the computed activation energy differed by about 7% (see Supporting Information, Figure S22). Thus, the value of 107 ± 1 kJ/mol for ESR-255 reported previously[90] does not reflect a significant difference. In neither the tricyanates nor their dicyanate analogs (see Supporting Information, Section S3) were any significant differences in activation energy found when considering the effect of substitution of Si for C in highly pure samples. Note that the absolute conversion rates observed did vary significantly among monomers and batches with differing purities (but not among highly purified batches of the same monomer), a reflection of the fact that the cyclotrimerization of cyanate esters are primarily determined by the nature of impurities.

In the case of dicyanates, the substitution of Si for C in the bridge linking the aryl cyanate groups in fully cyclotrimerized networks results in a significant decline in the glass transition temperature (from about 320 °C to 260 °C for BADCy and SiMCy, respectively, see Supporting Information Section S4). As a result, the ability to utilize SiMCy for very high temperature applications is more limited compared to BADCy. For the corresponding tricyanates, however, the mechanical softening points of sufficiently cyclotrimerized networks are so high that they are not a factor in limiting high temperature service, and thus substitution of more flexible Si-C bonds

for C-C bonds in the bridges connecting aryl cyanates does not adversely affect service temperatures. However, the tricyanate architecture studied comes with the significant drawback of an inability to achieve complete cyclotrimerization due to steric hindrance, which typically leads to decreased thermal and hydrolytic stability in cyanurate networks.

One way to overcome the aforementioned limitation is to cocure monomers such as Sicy-3 with other cyanate esters that can fully cyclotrimerize. Primaset® LECy, being a low viscosity liquid at room temperature and featuring a more flexible ethylidene bridge between two aryl cyanates, has long been recognized as an excellent choice for formulating multi-component cyanate ester mixtures, though formulation with other liquid dicyanates, such as RTX-366,[96,97] is also possible. We investigated the cocuring of SiCy-3 and its tetracyanate analog SiCy-4 with LECy. Figures 8 and 9 show non-isothermal DSC scans of SiCy-3 and SiCy-4, respectively, cocured with an equal weight of LECy. (For these preliminary investigations, purification by chromatography was not undertaken.)

The scans show clearly that the crystallization of the tri- or tetracyanate component is greatly curtailed, and the melting points lowered, by mixing with LECy. In addition, the cyclotrimerization exotherms are more symmetric, particularly for the SiCy-3 / LECy mixture, indicating more complete cyclotrimerization. The enthalpies of cyclotrimerization were 128 ± 13 kJ/eq. and 113 ± 11 kJ/eq. for the SiCy-3 and SiCy-4 mixtures, respectively, indicative of complete cyclotrimerization. Additional evidence for dramatic improvements in the ability to fully cyclotrimerize the mixtures is presented in Figure 10, which shows the FT-IR spectra of cured SiCy-3 and cocured SiCy-3 / LECy (mixed in equal weights) after 24 hours at 210 °C. Peaks near 2250 cm^{-1} due to residual unreacted cyanate ester groups are still clearly present in the neat SiCy-3 network, while in the cocured system the same peaks are almost completely absent.

The conversion to cyanurate is confirmed by the presence of the peaks near 1365 cm^{-1} and 1550 cm^{-1}.

Physical Properties of Cured Networks.

As mentioned earlier, the absence of a discernible glass transition in DSC scans of SiCy-3 and SiCy-4 (and their mixtures with LECy), suggests that a glass transition temperature in excess of 350 °C is possible for sufficiently cyclotrimerized networks. Previous studies of cyanate esters have shown that when such high glass transition temperatures are possible, the actual glass transition temperatures obtained during cure are primarily controlled by the cure temperature rather than the glass transition temperature of the fully cured network.[90] This principle is illustrated in Figure 11, which compares DSC traces of BADCy, SiMCy, ESR-255, and SiCy-3 after 12 hours at 210 °C in the DSC, followed by quenching (not shown) and re-heating (shown). For the dicyanates, the step change in heat capacity associated with the glass transition is clearly visible, and occurs between the cure temperature (210 °C) and the glass transition temperature at full cure (roughly 260 °C for SiMCy and 320 °C for BADCy). The difference in the "as cured" glass transition temperatures (which were 213 °C for SiMCy and 247 °C for BADCy) principally reflect the difference in the glass transition temperatures of the fully cured networks. In contrast, for both ESR-255 and SiCy-3, the "as cured" glass transition temperatures are between 275 °C and 280 °C, and are indicated by the onset of significant residual cure (as a result of de-vitrification) with the step change in heat capacity masked by the cure exotherm. The SiCy-3 appears to have a slightly higher de-vitrification temperature, which may simply reflect overall faster cure kinetics during the isothermal stage compared to ESR-255. The faster cure kinetics may allow more time for the network to cure very slowly once vitrified, thereby pushing the glass transition to a slightly higher temperature.

Analysis of the SiCy-3, SiCy-3 / LECy, and SiCy-4 / LECy networks was also undertaken by TMA (see Supporting Information, Section S5). The TMA scans confirmed that all three networks exhibited glass transition temperatures of at least 360 °C after heating to 350 °C. Thus, for the networks formed by cocuring with LECy, both full conversion and a very high glass transition temperature are possible, making these networks good candidates for dry high-temperature applications. Analysis of moisture uptake, however, revealed a significant weakness. The water uptake of the SiCy-3 network was 5.5%, while that of the SiCy-3 / LECy and SiCy-4 / LECy networks were 4.7% and 4.4%, respectively, after 96 hours immersion at 85 °C of networks cured for 24 hours at 210 °C). These values are significantly higher than either ESR-255 (3.5%) or ESR-255 cocured with an equal weight of LECy (2.7%). In order to determine the extent to which sample purity played a role in these results, the same water uptake test was performed on a sample of SiCy-3 further purified by chromatography. The resultant water uptake of 5.0% represents only a modest improvement, and is still much higher than the corresponding value for ESR-255. This result contrasts with earlier results for dicyanates[19] (confirmed by us in catalyzed networks)[17] that show significantly lower water uptake for SiMCy compared to BADCy under identical conditions.

In the dicyanate case, the lower glass transition temperature of SiMCy compared to BADCy is believed to be the key factor that drives the difference in water uptake. The lower glass transition temperature of SiMCy allows for greater relaxation of the free volume formed by cyclotrimerization during cure in the vitreous state, and thereby limits the capacity for water uptake. In fact, when cured at 250 °C, networks of uncatalyzed SiMCy (very close to the glass transition temperature) showed half the water uptake compared to networks of BADCy[19] (for which the glass transition temperature can be significantly higher). When catalyzed networks were cured at 210 °C (well below the glass transition temperature for both networks), the water uptake of SiMCy was only about 15% lower than that of BADCy.[17] Because the water uptake

values of fully cured cyanurate networks are typically quite similar whether catalyzed or not, the relaxation of free volume near the glass transition temperature appears to be the key factor. As mentioned earlier, the glass transition temperatures achieved by cure at 210 °C were slightly higher for SiCy-3 than for ESR-255, but both were much higher than the cure temperature. ESR-255, however, spent less time in the vitreous state due to its slower cure kinetics. These factors suggest the water uptake for the SiCy-3 networks should be higher than for ESR-255. Although the development of free volume during cure in the vitreous state may play an important role in determining the differences in water uptake[98] between networks containing SiCy-3 and ESR-255, a more detailed investigation would be needed to establish the cause with certainty.

As expected the higher water uptake for SiCy-3 and SiCy-3 / LECy networks leads to lower "wet" glass transition temperatures (202 °C and 226 °C, respectively) compared to their ESR-255 analogs (224 °C and 242 °C, respectively). The SiCy-4 / LECy network, however, equals the performance of the ESR-255 / LECy network, with a "wet" glass transition temperature (T_G) of 247 °C. The higher water uptake for the silicon-containing networks is expected to lead to faster hydrolytic degradation of the cyanurate networks. The unexpectedly high value of the "wet" T_G for the SiCy-4 / LECy network, however, is presently unexplained. It suggests that further exploration of the relationship between network functionality and moisture resistance in cyanurate networks could provide valuable insights that would enhance performance.

A final consideration is the thermochemical stability of the networks. In the dicyanate case, incorporation of Si into the network chains appeared to provide significant protection from oxidation at high temperatures, raising char yields in air to around 50%. As seen in Figures 12-14, TGA traces in nitrogen and air for SiCy-3, SiCy-3 / LECy (equal parts by weight), and SiCy-4 / LECy (equal parts by weight) networks, respectively, also show char yields in excess of 50% in both nitrogen and air, with the SiCy-4 / LECy network providing the best char yield in nitrogen

(70%) and similar char yields between 50-56% in air for all three networks. A full tabulation of all comparative data (along with graphical data for the ESR-255 / LECy networks) is provided in Supporting Information, Section S6. Interestingly, ESR-255 networks exhibited higher degradation onset temperatures and higher char yields compared to SiCy-3 networks, while the SiCy-3 / LECy networks showed lower degradation onset temperatures but higher char yields than the ESR-255 / LECy networks.

Taken together, these results indicate that in cases where there is a large difference in the thermochemical degradation of a network in air as compared to nitrogen, the presence of Si appears to provide a consistent improvement in char yield in air. The magnitude of the improvement at 600 °C is much larger than can be accounted for simply by the formation of non-volatile SiO_2 in place of volatile CO_2 with all else being equal whenever Si is substituted for C in the network structure, suggesting a true protective effect. However, when thermal degradation in air and under nitrogen are very similar, as is the case for many cyanurate networks with high char yields, then the presence of Si does not improve char yield significantly. Thus, the protective effect appears to be important only if oxidation provides a significant contribution to thermal degradation. Another important point to note is that, in comparison to cyanurate networks in which Si offers a significant protective effect, even higher char yields in air are readily obtained in cyanurate networks with no Si simply by avoiding functional groups (such as isopropylidene bridges between phenyl rings) that promote degradation.[90]

CONCLUSIONS

The synthesis of two new cyanate ester monomers, tris(4-cyanatophenyl)methylsilane and tetrakis(4-cyanatophenyl)silane, was achieved in overall yields of around 50% with good purity using a straightforward extension of a three-step method originally developed for the synthesis of bis(4-cyanatophenyl)dimethylsilane from diphenyldichlorosilane. The primary advantage of the

new tri- and tetra-functional cyanate ester monomers was the ability to achieve much higher glass transition temperatures (at least 350 °C) at the maximum practical extent of cure. As single-component networks, however, both monomers could not be completely converted to cyanurate due to steric hindrance of the uncured cyanate ester groups. Cocuring with an equal weight of the dicyanate monomer Primaset® LECy, however, enabled practically complete conversion to be obtained while maintaining a glass transition temperature in the fully cured state of over 350 °C. The higher melting points of the monomers, however, did limit the available processing window, to a modest extent for the neat tri-functional monomer (melting point 118 °C), and severely for the tetra-functional monomer (melting point 169 °C). Cocured systems, however, retained the favorable processing characteristics of di(cyanate ester) monomers. As with networks formed from di(cyanate ester) monomers, a significant improvement in thermo-oxidative stability compared to carbon-containing analogs was achieved for silicon-containing networks, but only in cases where oxidation contributed significantly to the thermal degradation. The water uptake for the silicon-containing networks was, in all cases, significantly higher compared to carbon-containing analogs, perhaps due to differences in the evolution of free volume during cure. The higher water uptake leads to a lower "wet" T_G in the silicon-containing networks when compared to their carbon-containing analogs. Nonetheless, the "wet" T_G, at 247 °C, of the best performing networks, produced by cocuring the tetrakis(cyanate ester) silane with Primaset® LECy, represents outstanding "wet" performance in an easily processed thermosetting resin.

ACKNOWLEDGEMENTS

The support of the Air Force Office of Scientific Research is gratefully acknowledged. CMS performed this work as part of the National Research Council Research Associateship Program.

REFERENCES AND NOTES

1. Chemistry and Technology of Cyanate Ester Resins; Hamerton, I., Ed.; Chapman & Hall: London, **1994**.

2. Nair, C. P. R.; Mathew, D.; Ninan, K. N. In New Polymerization Techniques and Synthetic Methodologies; Abe, A., Albertsson, A.-C., Cantow, H. J., Eds.; Advances in Polymer Science 155; Springer: New York, **2001**; pp 1-99.
3. Fang, T.; Shimp, D. A. *Prog. Polym. Sci.* **1995,** *20*, 61-118.
4. Hamerton, I.; Hay, J. N. *High Perform. Polym.* **1998,** *10*, 163-174.
5. Fabian, P.; Haynes, M.; Babcock, H.; Hooker, M. *IEEE Trans. Appl. Supercond.* **2013,** *23*, No. 7700204.
6. Munshi, N. A.; Walsh, J. K.; Hooker, M. W.; Babcock, H. K.; Haight, A. H.; Durso, S. R.; Kawaguchi, A.; Hough, P. *IEEE Trans. Appl. Supercond.* **2013,** *23*, No. 7700104.
7. Abramian, P.; de Aragon, F.; Calero, J.; de la Gama, J.; Garcia-Tabares, L.; Gutierrez, J. L.; Karppinen, M.; Martinez, T.; Rodriguez, E.; Rodriguez, I.; Sanchez, L.; Toral, F.; Vazquez, C. *IEEE Trans. Appl. Supercond.* **2013,** *23*, No. 4101204.
8. Chen, H. C.; Shivakumar, K. *CMC-Comput. Mat. Contin.* **2008,** *8*, 33-42.
9. Shivakumar, K. N.; Chen, H.; Holloway, G. *J. Reinf. Plast. Compos.* **2009,** *28*, 675-689.
10. Chen, P. C.; Bowers, C. W.; Content, D. A.; Marzouk, M.; Romeo, R. C. *Opt. Eng.* **2000,** *39*, 2320-2329.
11. Wienhold, P. D.; Persons, D. F. *SAMPE J.* **2003,** *39*, 6-17.
12. Lyon, R. E.; Walters, R. N.; Gandhi, S. *Fire Mater.* **2006,** *30*, 89-106.
13. Yan, H. X.; Zhang, M. M.; Liu, C.; Zhang, J. P. *Polym. Bull.* **2013,** *70*, 2923-2933.
14. Zhang, Z. Y.; Gu, A. J.; Liang, G. Z.; Yuan, L.; Zhuo, D. X. *Soft Mater.* **2013,** *11*, 346-352.
15. Yu, H.; Shen, C. J.; Tian, M. Z.; Qu, J.; Wang, Z. G. *Macromolecules* **2012,** *45*, 5140-5150.
16. Reams, J. T.; Guenthner, A. J.; Lamison, K. R.; Vij, V.; Lubin, L. M.; Mabry, J. M. *ACS Appl. Matl. Interfaces* **2012**, *4*, 527-535.
17. Guenthner, A. J.; Lamison, K. R.; Vij, V.; Reams, J. T.; Yandek, G. R.; Mabry, J. M. *Macromolecules* **2012**, *45*, 211-220.
18. Zhuo, D. X.; Gu, A. J.; Liang, G. Z.; Hu, J. T.; Cao, L.; Yuan, L. *Polym. Degrad. Stab.* **2011,** *96*, 505-514.
19. Guenthner, A. J.; Yandek, G. R.; Wright, M. E.; Petteys, B. J.; Quintana, R.; Connor, D.; Gilardi, R. D.; Marchant, D. *Macromolecules* **2006,** *39*, 6046-6053.
20. Wright, M. E., *Polym. Prepr. (Am. Chem. Soc., Div. Polym. Chem.)* **2004,** *45 (2)*, 294.
21. Maya, E. M.; Snow, A. W.; Buckley, L. J. *Macromolecules* **2002,** *35*, 460-466.
22. Zaldivar, R. J.; Salfity, J.; Steckel, G.; Morgan, B.; Patel, D.; Nokes, J. P.; Kim, H. I. *J. Compos. Mater.* **2012,** *46*, 1925-1936.
23. Dai, S. K.; Gu, A. J.; Liang, G. Z.; Yuan, L. *Polym. Adv. Technol.* **2011,** *22*, 262-269.
24. Pollack, S. K.; Fu, Z. *Polym. Prepr. (Am. Chem. Soc., Div. Polym. Chem.)* **1998,** *39*, 452-453.
25. Devaraju, S.; Vengatesan, M. R.; Selvi, M.; Song, J. K.; Alagar, M. *Microporous Mesoporous Mater.* **2013,** *179*, 157-164.
26. Wu, G. L.; Kou, K. C.; Chao, M.; Zhuo, L. H.; Zhang, J. Q. *J. Wuhan Univ. Technol.-Mat. Sci. Edit.* **2013,** *28*, 261-264.
27. Sun, W. X.; Sun, W. Z.; Kessler, M. R.; Bowler, N.; Dennis, K. W.; McCallum, R. W.; Li, Q.; Tan, X. L. *ACS Appl. Matl. Interfaces* **2013,** *5*, 1636-1642.
28. Taha, E. A.; Wu, J. T.; Gao, K.; Guo, L. *Chin. J. Polym. Sci.* **2012,** *30*, 530-536.
29. Hu, J. T.; Gu, A. J.; Liang, G. Z.; Zhuo, D. X.; Yuan, L. *Polym. Adv. Technol.* **2012,** *23*, 454-462.

30. Sheng, X.; Akinc, M.; Kessler, M. R. *Polym. Eng. Sci.* **2010,** *50*, 1075-1084.
31. Goertzen, W. K.; Kessler, M. R. *J. Appl. Polym. Sci.* **2008,** *109*, 647-653.
32. Goertzen, W. K.; Kessler, M. R. *J. Therm. Anal. Calorim.* **2008,** *93*, 87-93.
33. Zhang, Q. L.; Ma, X. Y.; Liang, G. Z.; Qu, X. H.; Huang, Y.; Wang, S. H.; Kou, K. C. *J. Polym. Sci., Part B: Polym. Phys.* **2008,** *46*, 1243-1251.
34. Goertzen, W. K.; Sheng, X.; Akinc, M.; Kessler, M. R. *Polym. Eng. Sci.* **2008,** *48*, 875-883.
35. Goertzen, W. K.; Kessler, M. R., *Commposites, Part A* **2008,** *39*, 761-768.
36. Wooster, T. J.; Abrol, S.; MacFarlane, D. R. *Macromol. Mater. Eng.* **2005,** *290*, 961-969.
37. Wooster, T. J.; Abrol, S.; Hey, J. M.; MacFarlane, D. R. *Macromol. Mater. Eng.* **2004,** *289*, 872-879.
38. Wooster, T. J.; Abrol, S.; Hey, J. M.; MacFarlane, D. R. *Composites, Part A* **2004,** *35*, 75-82.
39. Lin, Y.; Song, M.; Stone, C. A.; Shaw, S. J. *Thermochim. Acta* **2013,** *552*, 77-86.
40. Yuan, L.; Gu, A. J.; Liang, G. Z.; Ma, X. Y.; Lin, C.; Chen, F. *Polym. Eng. Sci.* **2012,** *52*, 2443-2453.
41. John, B.; Nair, C. P. R.; Ninan, K. N. *Mater. Sci. Eng., A* **2010,** *527*, 5435-5443.
42. Kissounko, D. A.; Deitzel, J. M.; Doherty, S. P.; Shah, A.; Gillespie, J. W. *Eur. Polym. J.* **2008,** *44*, 2807-2819.
43. Nagendiran, S.; Chozhan, C. K.; Alagar, M.; Hamerton, I. *High Perform. Polym.* **2008,** *20*, 323-347.
44. Anthoulis, G. I.; Kontou, E.; Fainleib, A.; Bei, I.; Gomza, Y. *J. Polym. Sci., Part B: Polym. Phys.* **2008,** *46*, 1036-1049.
45. Bershtein, V. A.; Fainleib, A. M.; Pissis, P.; Bei, I. M.; Dalmas, F.; Egorova, L. M.; Gomza, Y. P.; Kripotou, S.; Maroulos, P.; Yakushev, P. N. *J. Macromol. Sci., Part B: Phys.* **2008,** *47*, 555-575.
46. Fang, Z. P.; Shi, H. H.; Gu, A. J.; Feng, Y. *J. Mater. Sci.* **2007,** *42*, 4603-4608.
47. Yu, D. H.; Wang, B.; Feng, Y.; Fang, Z. P. *J. Appl. Polym. Sci.* **2006,** *102*, 1509-1515.
48. Mondragon, I.; Solar, L.; Nohales, A.; Vallo, C. I.; Gomez, C. M. *Polymer* **2006,** *47*, 3401-3409.
49. Wooster, T. J.; Abrol, S.; MacFarlane, D. R.. *Polymer* **2005,** *46*, 8011-8017.
50. Feng, Y.; Fang, Z. P.; Mao, W.; Gu, A. J. *J. Appl. Polym. Sci.* **2005,** *96*, 632-637.
51. Wooster, T. J.; Abrol, S.; MacFarlane, D. R., *Polymer* **2004,** *45*, 7845-7852.
52. Ganguli, S.; Dean, D.; Jordan, K.; Price, G.; Vaia, R. *Polymer* **2003,** *44*, 6901-6911.
53. Ganguli, S.; Dean, D.; Jordan, K.; Price, G.; Vaia, R. *Polymer* **2003,** *44*, 1315-1319.
54. Devaraju, S.; Vengatesan, M. R.; Selvi, M.; Kumar, A. A.; Hamerton, I.; Go, J. S.; Alagar, M. *RSC Adv.* **2013,** *3*, 12915-12921.
55. Zhuo, D. X.; Gu, A. J.; Wang, Y. Z.; Liang, G. Z.; Hu, J. T.; Yuan, L.; Yao, W. *Polym. Adv. Technol.* **2012,** *23*, 1121-1128.
56. Zhan, G. Z.; Tang, X. L.; Yu, Y. F.; Li, S. J. *Polym. Eng. Sci.* **2011,** *51*, 426-433.
57. Zhuo, D. X.; Gu, A. J.; Liang, G. Z.; Hu, J. T.; Yuan, L. *J. Mater. Sci.* **2011,** *46*, 1571-1580.
58. Jothibasu, S.; Kumar, A. A.; Alagar, M. *High Perform. Polym.* **2011,** *23*, 11-21.
59. Pan, Y. Z.; Xu, Y.; An, L.; Lu, H. B.; Yang, Y. L.; Chen, W.; Nutt, S. *Macromolecules* **2008,** *41*, 9245-9258.
60. Lin, R. H.; Lin, C. W.; Lee, A. C.; Chen, Y. H.; Yen, F. S. *J. Appl. Polym. Sci.* **2007,** *103*, 1356-1366.

61. Zhang, Z. P.; Liang, G. Z.; Wang, X. L.; Adhikari, S.; Pei, J. Z. *High Perform. Polym.* **2013,** *25*, 427-435.
62. Rakesh, S.; Dharan, C. P. S.; Selladurai, M.; Sudha, V.; Sundararajan, P. R.; Sarojadevi, M.,. *High Perform. Polym.* **2013,** *25*, 87-96.
63. Jothibasu, S.; Devaraju, S.; Venkatesan, M. R.; Chandramohan, A.; Kumar, A. A.; Alagar, M. *High Perform. Polym.* **2012,** *24*, 379-388.
64. Chandramohan, A.; Dinkaran, K.; Kumar, A. A.; Alagar, M., *High Perform. Polym.* **2012,** *24*, 405-417.
65. Hu, J. T.; Gu, A. J.; Jiang, Z. J.; Liang, G. Z.; Zhuo, D. X.; Yuan, L.; Zhang, B. J.; Chen, X. X. *Polym. Adv. Technol.* **2012,** *23*, 1219-1228.
66. Zhang, Z. P.; Pei, J. Z.; Liang, G. Z.; Yuan, L. *J. Appl. Polym. Sci.* **2011,** *121*, 1004-1012.
67. Lin, Y.; Jin, J.; Song, M.; Shaw, S. J.; Stone, C. A. *Polymer* **2011,** *52*, 1716-1724.
68. Hu, J. T.; Gu, A. J.; Liang, G. Z.; Zhuo, D. X.; Yuan, L. *J. Appl. Polym. Sci.* **2011,** *120*, 360-367.
69. Liang, K.; Toghiani, H.; Pittman, C. U. *J. Inorg. Organomet. Polym. Mater.* **2011,** *21*, 128-142.
70. Wright, M. E.; Petteys, B. J.; Guenthner, A. J.; Yandek, G. R.; Baldwin, L. C.; Jones, C.; Roberts, M. J. *Macromolecules* **2007,** *40*, 3891-3894.
71. Liang, K. W.; Li, G. Z.; Toghiani, H.; Koo, J. H.; Pittman, C. U. *Chem. Mater.* **2006,** *18*, 301-312.
72. Lu, T. L.; Liang, G. Z.; Guo, Z. *J. Appl. Polym. Sci.* **2006,** *101*, 3652-3658.
73. Wright, M. E.; Petteys, B. J.; Guenthner, A. J.; Fallis, S.; Yandek, G. R.; Tomczak, S. J.; Minton, T. K.; Brunsvold, A. *Macromolecules* **2006,** *39*, 4710-4718.
74. Cho, H. S.; Liang, K. W.; Chatterjee, S.; Pittman, C. U. *J. Inorg. Organomet. Polym. Mater.* **2005,** *15*, 541-553.
75. Liang, K. W.; Toghiani, H.; Li, G. Z.; Pittman, C. U. *J. Polym. Sci., Part A: Polym. Chem.* **2005,** *43*, 3887-3898.
76. Duo, S. W.; Song, M. M.; Liu, T. Z.; Hu, C. Y.; Li, M. S. *J. Nanosci. Nanotechnol.* **2013,** *13*, 1356-1359.
77. Minton, T. K.; Wright, M. E.; Tomczak, S. J.; Marquez, S. A.; Shen, L. H.; Brunsvold, A. L.; Cooper, R.; Zhang, J. M.; Vij, V.; Guenthner, A. J.; Petteys, B. J. *ACS Appl. Matl. Interfaces* **2012,** *4*, 492-502.
78. Zhang, X. W.; Ren, H. Y.; Wang, J. H.; Zhang, Y.; Shao, Y. Y. *Mater. Lett.* **2011,** *65*, 821-824.
79. Cheng, X. E.; Shi, W. F. *J. Therm. Anal. Calorim.* **2011,** *103*, 303-310.
80. Hsiue, G. H.; Wang, W. J.; Chang, F. C.. *J. Appl. Polym. Sci.* **1999,** *73*, 1231-1238.
81. Park, S. J.; Jin, F. L.; Lee, J. R. *Macromol. Res.* **2005**, *13*, 8-13.
82. Thulasiraman, V.; Sarojadevi, M. *High Perform. Polym.* **2009,** *21*, 437-454.
83. Wang, W. J.; Perng, L. H.; Hsiue, G. H.; Chang, F. C. *Polymer* **2000,** *41*, 6113-6122.
84. Liu, Y. L.; Hsu, C. W.; Chou, C. I. *J. Polym. Sci., Part A: Polym. Chem.* **2007,** *45*, 1007-1015.
85. Chiang, C. Y.; Tsai, R. S.; Shu, W. J. *e-Polym.* **2007**, *7*, 1499-1512**.**
86. Tang, H. Y.; Song, N. H.; Chen, X. F.; Fan, X. H.; Zhou, Q. F.. *J. Appl. Polym. Sci.* **2008,** *109*, 190-199.
87. Tsai, R. S.; Wang, Z. Y.; Shu, W. J. *Int. Polym. Proc.* **2010,** *25*, 125-131.
88. Guenthner, A. J.; Davis, M. C.; Lamison, K. R.; Yandek, G. R.; Cambrea, L. R.; Groshens, T. J.; Baldwin, L. C.; Mabry, J. M. *Polymer* **2011,** *52*, 3933-3942.

89. Shimp, D. A.; Ising, S. J.; Christenson, J. R. In High Temperature Polymers and Their Uses; Society of Plastics Engineers: Cleveland, OH, 1989; pp 127-140.
90. Guenthner, A. J.; Davis, M. C.; Ford, M. D.; Reams, J. T.; Groshens, T. J.; Baldwin, L. C.; Lubin, L. M.; Mabry, J. M. *Macromolecules* **2012**, *45*, 9707-9718.
91. Reams, J. T. Ph. D. Dissertation, South Dakota School of Mines, Rapid City, SD, 2011.
92. Guenthner, A. J.; Reams, J. T.; Lamison, K. R.; Ramirez, S. M.; Swanson, D. D.; Yandek, G. R.; Sahagun, C. M.; Davis, M. C.; Mabry, J. M. *ACS Appl. Matl. Interfaces* **2013**, *5*, 8772-8783.
93. Guenthner, A. J.; Yandek, G. R.; Mabry, J., M; Lamison, K. R.; Vij, V.; Davis, M. C.; Cambrea, L. R. Insights into moisture uptake and processability from new cyanate ester monomer and blend studies. SAMPE International Technical Conference; SAMPE International Business Office: Covina, CA, 2010; paper 42ISTC-119.
94. Kamal, M. R.; Sourour, S. *Polym. Eng. Sci*. **1973**, *13*, 59-64.
95. Kenny, J. M. *J. Appl. Polym. Sci.* **1994**, *51*, 761-764.
96. Simon, S. L.; Gillham, J. K. *J. Appl. Polym. Sci.* **1993**, *47*, 461-485.
97. Shimp, D. A.; Ising, S. J. In Advanced materials: the challenge for the next decade: 35th International SAMPE Symposium and Exhibition; Janicki, G.; Bailey, V.; Schjelderup, H., Eds.; SAMPE International Business Office, Covina, CA, 1990; p. 1045.
98. Georjon, O.; Galy, J. *Polymer* **1998**, *39*, 339-345.

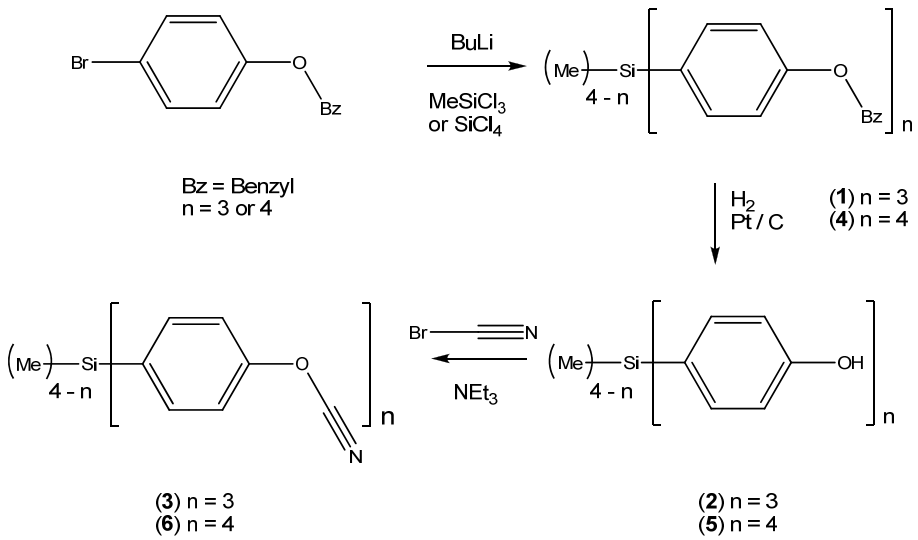

SCHEME 1 Synthesis of new cyanate ester derivatives SiCy-3 (**3**) and SiCy-4 (**6**)

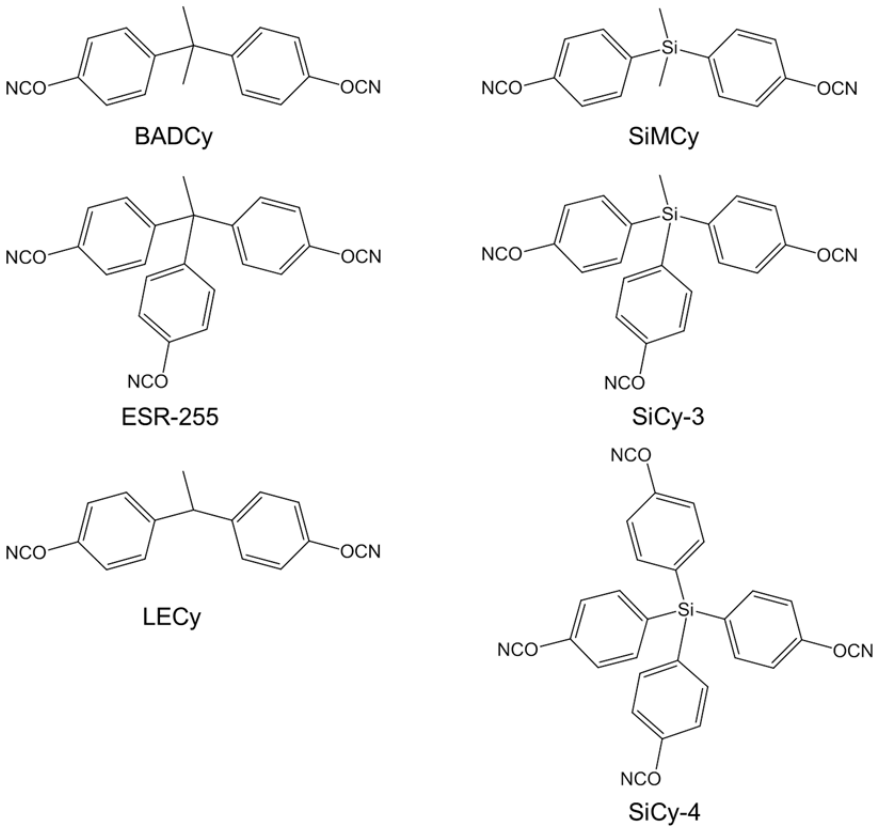

FIGURE 1 Chemical structure of monomers utilized for comparative studies

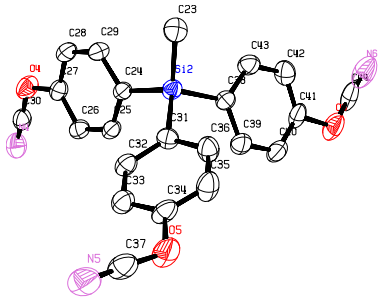

FIGURE 2 ORTEP representation of SiCy-3 (**3**) collected at 100K. Thermal ellipsoids shown at 50%. Hydrogen atoms omitted for clarity. Black, C; Blue, Si, Red, O; Purple, N

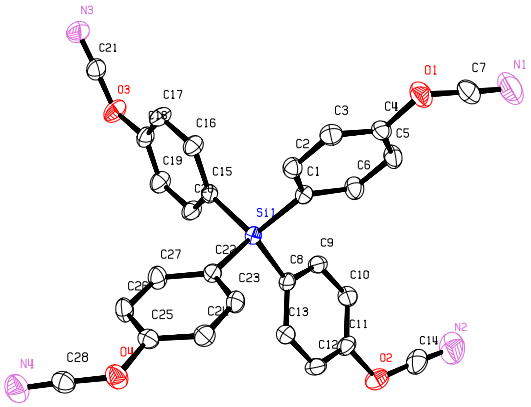

FIGURE 3 ORTEP representation of SiCy-4 (**6**) collected at 100K. Thermal ellipsoids shown at 50%. Hydrogen atoms omitted for clarity. Black, C; Blue, Si, Red, O; Purple, N

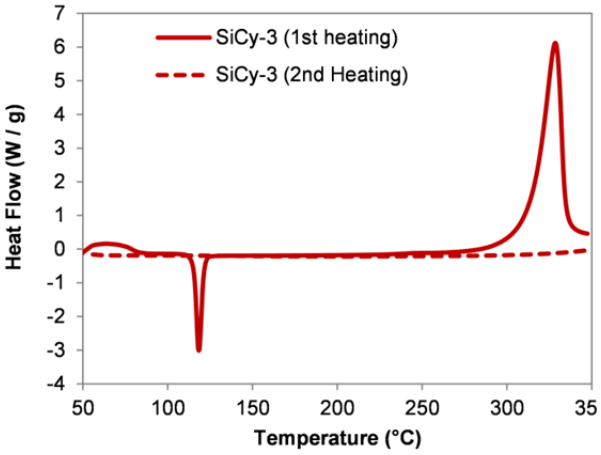

FIGURE 4 Non-isothermal DSC of SiCy-3 (**3**)

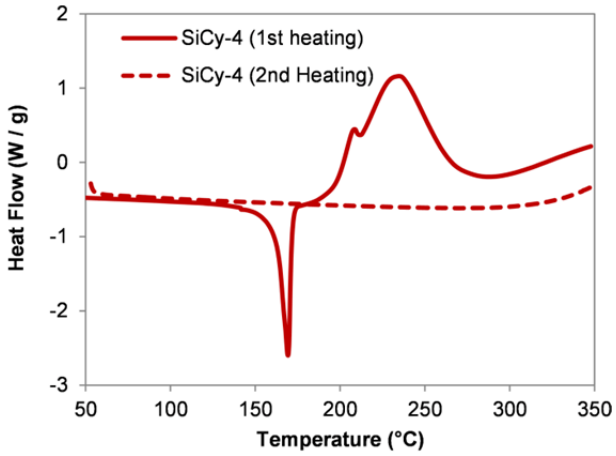

FIGURE 5 Non-isothermal DSC of SiCy-4 (**6**)

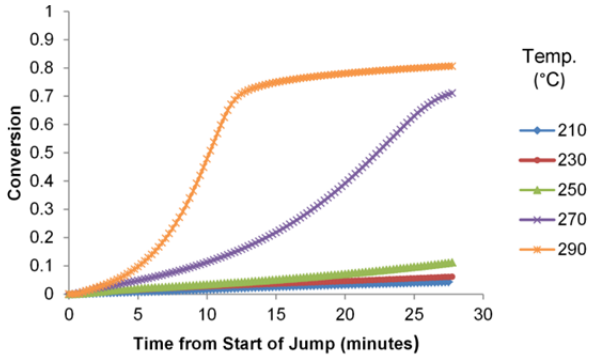

FIGURE 6 Isothermal cure kinetics of SiCy-3 (**3**) after purification by flash chromatography

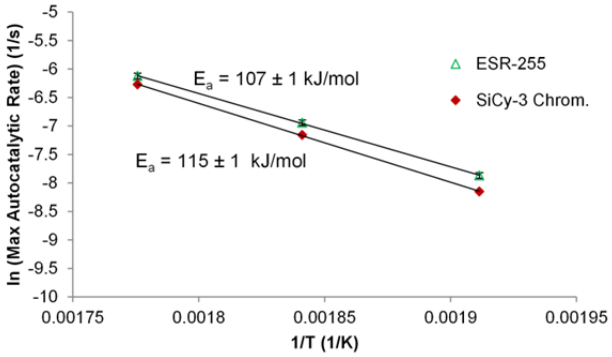

FIGURE 7 Arrhenius plot showing maximum auto-catalytic reaction rates of SiCy-3 (**3**, purified by chromatography) and ESR-255

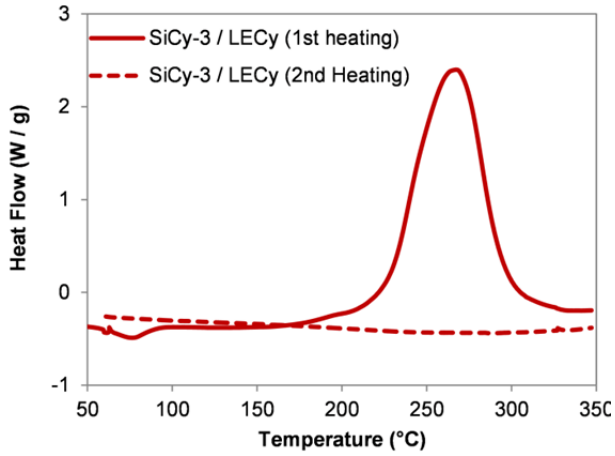

FIGURE 8 Non-isothermal DSC of SiCy-3 (**3**) cocured with an equal weight of LECy

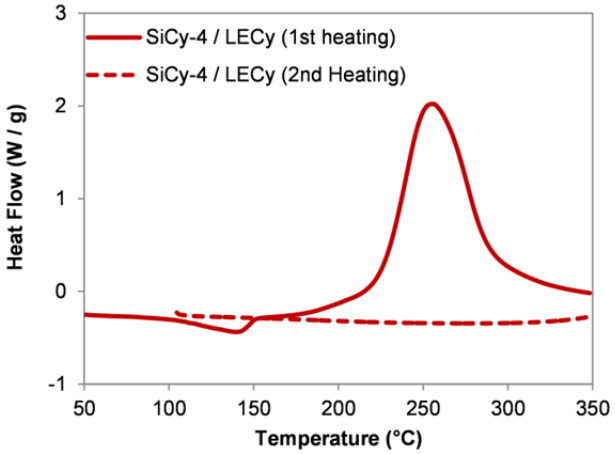

FIGURE 9 Non-isothermal DSC of SiCy-4 (**6**) cocured with an equal weight of LECy

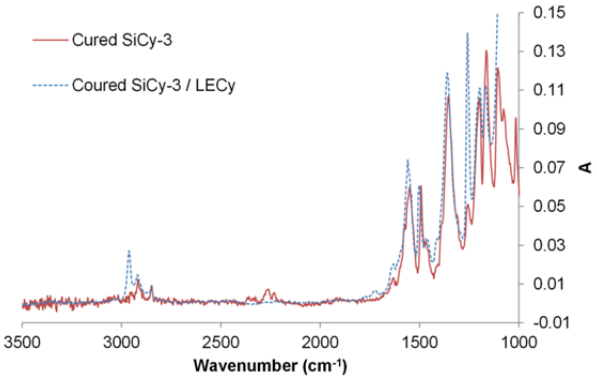

FIGURE 10 FT-IR spectra of SiCy-3 (**3**) and a mixture of equal parts SiCy-3 and LECy, after cure for 24 hours at 210 °C

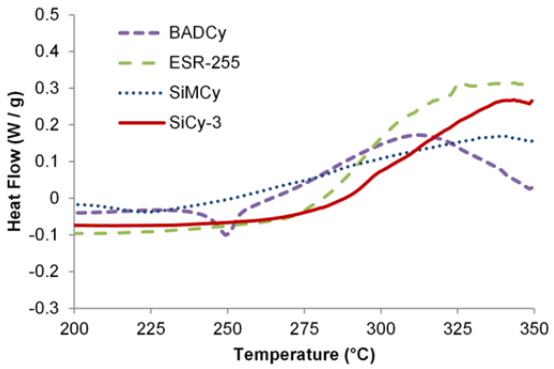

FIGURE 11 DSC scans after cure for 12 hours at 210 °C of SiCy-3 (**3**) compared to its carbon-containing analog ESR-255, and the respective silicon- and carbon-containing dicyanate analogs SiMCy and BADCy. The onset of residual cure at around 275-280 °C provides an indication of the T_G after the 12 hour cure for the tricyanates, while for the dicyanates, a step change in heat capacity (combined with an endothermic event for BADCy) indicates the T_G.

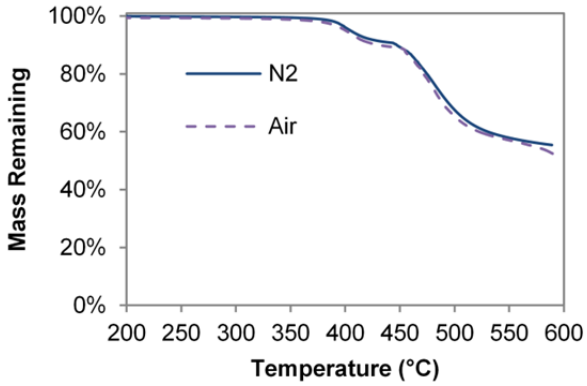

FIGURE 12 TGA traces of cured SiCy-3 (**3**) in nitrogen and air

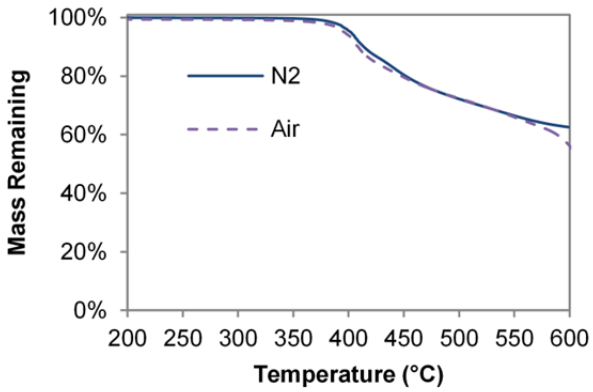

FIGURE 13 TGA traces of cured SiCy-3 (**3**) / LECy (mixed in equal parts by weight prior to cure) in nitrogen and air

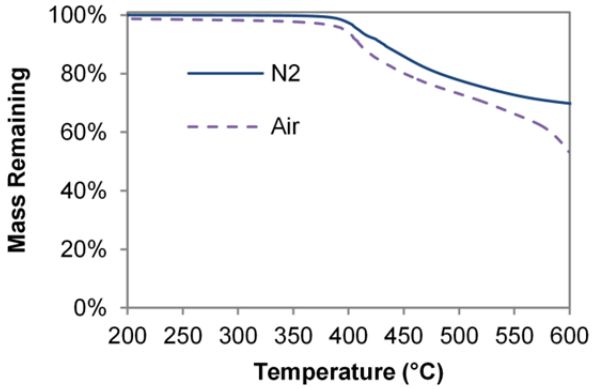

FIGURE 14 TGA traces of cured SiCy-4 (**6**) / LECy (mixed in equal parts by weight prior to cure) in nitrogen and air

TABLE 1 Key Thermo-Mechanical Properties of Networks Containing SiCy-3 (**3**) and SiCy-4 (**6**) Cured for 24 hr at 210 °C

Network[a]	Density (g/cc)	"Fully Cured" T_G (by TMA, °C)	Water Uptake (wt%)	"Wet" T_G (by TMA, °C)
SiCy-3	1.245	>360	5.5	202
SiCy-3 / LECy (50 / 50 wt%)	1.226	>360	4.4	226
SiCy-4 / LECy (50 / 50 wt%)	1.258	>360	4.7	247

[a] Density, water uptake, and "wet" T_G are for networks after 24 hours of cure at 210 °C

GRAPHICAL ABSTRACT

Authors: Andrew J. Guenthner, Vandana Vij, Timothy S. Haddad, Josiah T. Reams, Kevin R. Lamison, Christopher M. Sahagun, Sean M. Ramirez, Gregory R. Yandek, Suresh C. Suri, and Joseph M. Mabry

Title: Silicon-Containing Tri- and Tetra-Functional Cyanate Esters: Synthesis, Cure Kinetics, and Network Properties

Text: Two new cyanate ester monomers containing silicon can either be cured as neat monomers, or cocured with the dicyanate ester of Bisphenol E, to produce high-performance polycyanurate networks with glass transition temperatures in excess of 350 °C under dry conditions, and up to about 250 °C under wet conditions. The presence of silicon affords some protection against oxidation at elevated temperatures, while cocured networks also offer desirable processing and cure characteristics.

GRAPHICAL ABSTRACT FIGURE

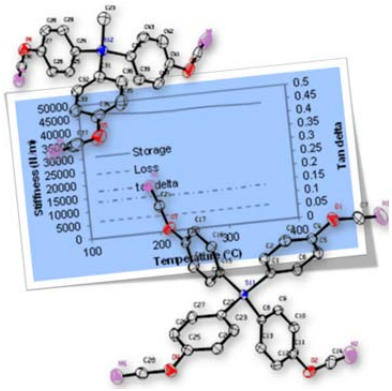

Supporting Information

"Silicon-Containing Tri- and Tetra-Functional Cyanate Esters: Synthesis, Cure Kinetics, and Network Properties"

Andrew J. Guenthner,[1] Vandana Vij,[2] Timothy S. Haddad,[2] Josiah T. Reams,[2] Kevin R. Lamison,[2] Christopher M. Sahagun,[3] Sean M. Ramirez,[2] Gregory R. Yandek,[1] Suresh C. Suri,[1] and Joseph M. Mabry[1]

[1] Aerospace Systems Directorate, Air Force Research Laboratory, Edwards AFB, CA 93524

[2] ERC Incorporated, Air Force Research Laboratory, Edwards AFB, CA 93524

[3] National Research Council / Air Force Research Laboratory, Edwards AFB, CA 93524

Correspondence to: Andrew J. Guenthner (E-mail: *andrew.guenthner@us.af.mil*)

S1. Samples Supplied for Comparison

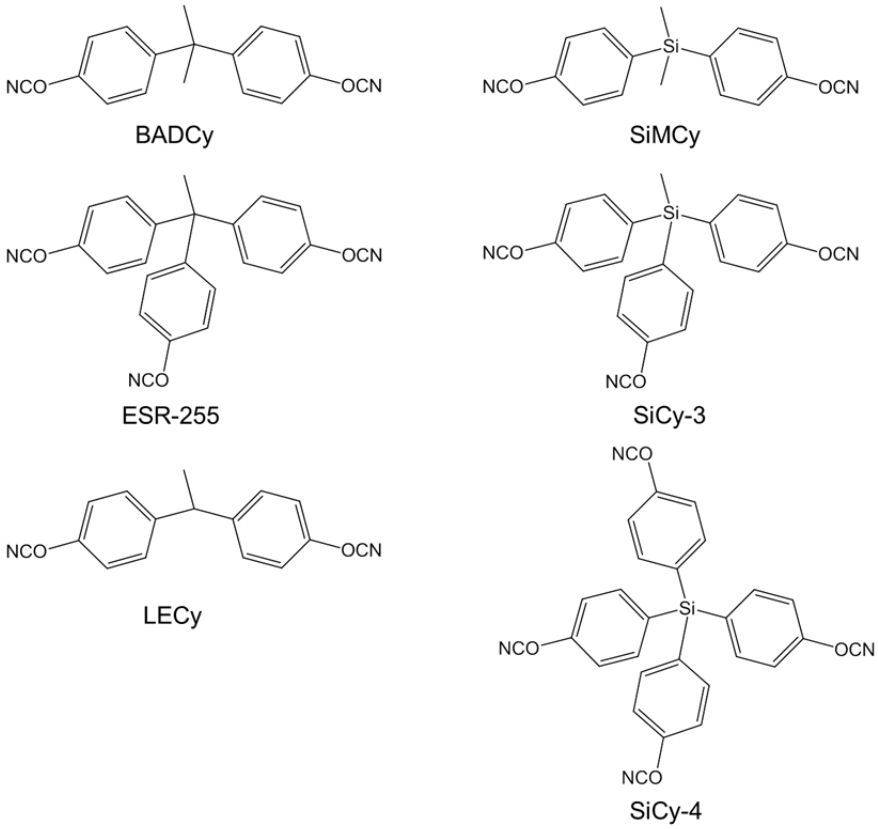

FIGURE S1. Chemical structure of monomers utilized for comparative studies.

TABLE S1 Nomenclature and Description of Samples Listed in Tables S2 – S10.

Monomer	Central Atom	*f*	Purification[a]	Description
BADCy	C	2	As-Rec'd	Commercial product; supplied by Lonza; carbon analog of SiMCy; portions of the data for BADCy have been reported in Supporting Information of previous publications[S1]
ESR-255	C	3	As-Rec'd	Experimental product reported by Shimp;[S2] synthesized at NAWCWD;[S3] carbon analog of SiCy-3; tri-functional analog of BADCy; portions of the data have been reported in previous publications[S3]
SiMCy	Si	2	Chrom.	Synthesized at AFRL;[S4] Si-analog of BADCy; di-functional analog of SiCy-3
SiCy-3	Si	3	Chrom.	Monomer (3) reported in main manuscript
SiCy-4	Si	4	As-Synth.	Monomer (6) reported in main manuscript; tetra-functional analog of SiCy-3
SiCy-3 B2	Si	3	Chrom	Second highly purified batch of SiCy-3; prepared to determine reproducibility of characterization data
SiMCy	Si	2	As-Synth.	As used for previous studies of catalyzed system[S4,S5]; uncatalyzed TGA data previously reported by Guenthner et al.[S6]
SiCy-3	Si	3	As-Synth.	Monomer (3) reported in main manuscript; prepared to determine effect of monomer purity on properties
SiCy-3 / LECy	Si	3 / 2	As-Synth.	50 wt% Monomer (3) cocured with 50 wt% LECy (LECy used as-supplied by Lonza)
SiCy-4 / LECy	Si	4 / 2	As-Synth.	50 wt% Monomer (6) cocured with 50 wt% LECy (LECy used as-supplied by Lonza)
ESR-255 / LECy	C	3 / 2	As-Synth.	50 wt% ESR-255 cocured with 50 wt% LECy (LECy used as-supplied by Lonza)

[a] Purification descriptions: "As Rec-d" = used as received; "As-Synth." = used after synthesis as described in Experimental section without further purification; "Chrom." = used after synthesis and further purification via flash chromatography as described in Experimental section.

S2. Non-Isothermal DSC Data

TABLE S2 Comparative Non-Isothermal DSC Parameters of Cyanate Ester Monomers

Monomer	Central Atom	f	Purity	$\Delta H_{Non\text{-}iso\ cure}$ [a] (J/g)	$\Delta H_{Non\text{-}iso\ cure}$ [a] (kJ/eq.)	$T_{Cure\text{-}Onset}$ (°C)	$T_{Cure\text{-}Peak}$ (°C)	$T_{G,Post\text{-}Cure}$ [b] (°C)
BADCy	C	2	As-Rec'd	749 ± 43	104 ± 6	312 ± 7	332	305
ESR-255	C	3	As-Rec'd	751 ± 36	95 ± 7	281 ± 11	311	>340[c]
SiMCy	Si	2	Chrom.	753 ± 22	111 ± 3	309 ± 3	336	248[d]
SiCy-3	Si	3	Chrom.	707 ± 27	94 ± 4	311 ± 6	328	>340[c]
SiCy-4	Si	4	As-Synth.	767 ± 79[e]	96 ± 10[e]	196 ± 2	225	>340[c]
SiCy-3 B2	Si	3	Chrom	756 ± 97	100 ± 12	312 ± 1	330	>340[c,f]
SiMCy	Si	2	As-Synth.	750 ± 37	110 ± 5	246 ± 1, 295 ± 4[g]	327	216[d]
SiCy-3	Si	3	As-Synth.	712 ± 36	94 ± 5	217 ± 1, 278 ± 5[g]	309	>340[c]
SiCy-3 / LECy	Si	3 / 2	As-Synth.	967 ± 101[e]	128 ± 13[e]	229 ± 7	267	>340[c]
SiCy-4 / LECy	Si	4 / 2	As-Synth.	873 ± 89[e]	112 ± 11[e]	224 ± 5	256	>340[c]
ESR-255 / LECy	C	3 / 2	As-Rec'd	852 ± 91[e]	110 ± 12[e]	290 ± 6	314	>340[c]

[a] Non-iso cure refers to cure observed on heating to 350 °C in the DSC except as noted; these values do not necessarily represent the total enthalpy of cyclotrimerization for the monomer to reach complete conversion; errors are those associated with the individual measurement, based on uncertainty in the baseline (these differ from the errors reported in Table S3, which are based on the sample statistics from multiple isothermal and non-isothermal DSC runs) [b] These values do not necessarily represent the value of T_G at full conversion ($T_{G\infty}$), which may be greater than the decomposition temperature [c] No T_G was observed by DSC below 340 °C [d] After heating run that terminated at a temperature of 360 °C [e] These samples do not have no internal calibration to correct weighing errors, therefore the error reflects uncertainties in both baseline and sample weight [f] After heating run that terminated at a temperature of 375°C [g] Exotherm showed two peaks, a small peak at the lower onset temperature, and a much larger peak at the higher onset temperature

TABLE S3 Comparative Melting Endotherm Analysis of Cyanate Ester Monomers

Monomer	Central Atom	*f*	Purification	# of Samples	T_m[a,b] (°C)	ΔH_m[b] (J/g)	Von t'Hoff Purity (%)
BADCy	C	2	As-Rec'd	6	82.8 ± 0.2	105 ± 9	99.2 ± 0.2
ESR-255[c]	C	3	As-Rec'd	19	115.3 ± 0.3	72 ± 4	99.4 ± 0.2
SiMCy	Si	2	Chrom.	5	60.3 ± 0.1	93 ± 1	99.4 ± 0.1
SiCy-3	Si	3	Chrom.	6	118.1 ± 0.1	74 ± 2	99.21 ± 0.04
SiCy-4	Si	4	As-Synth.	1	169.3	94	89.7
SiCy-3 B2[c]	Si	3	Chrom	10	117.8 ± 0.1	76 ± 1	99.38 ± 0.09
SiMCy	Si	2	As-Synth.	6	60.3 ± 0.1	89 ± 4	96.0 ± 0.4
SiCy-3	Si	3	As-Synth.	7	115.6 ± 0.5	69 ± 3	96.0 ± 0.6
SiCy-3 / LECy	Si	3 / 2	As-Synth.	1	75.7	26	n/a
SiCy-4 / LECy	Si	4 / 2	As-Synth.	1	139.6	30	n/a
ESR-255 / LECy	C	3 / 2	As-Rec'd	1	64.3	22	n/a

[a] Temperature of peak endothermic heat flow [b] Values are not corrected based on von t'Hoff analysis; note that for mixed monomers, the degree of crystallinity is likely much less than predicted by a simple rule of mixtures.[c] Data originally reported in Supporting Information of Reference S3

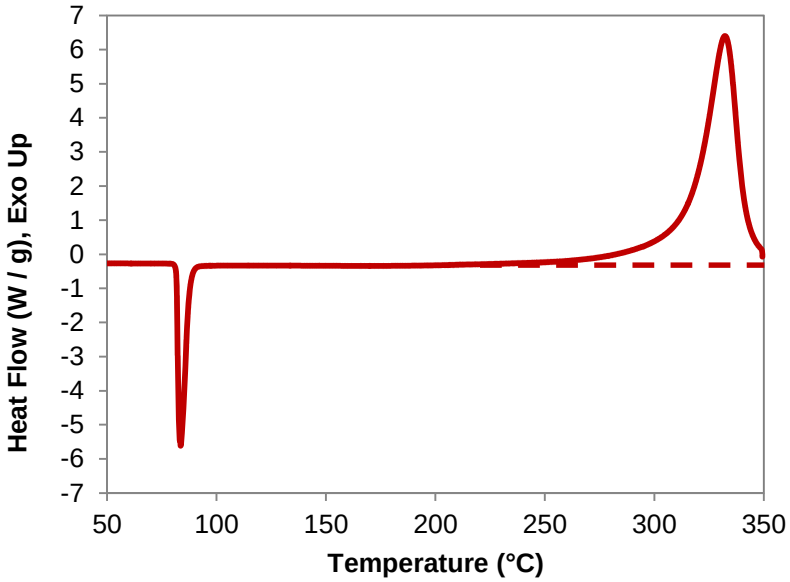

FIGURE S2. Non-isothermal DSC of BADCy (originally published in Ref S1, Supporting Information, used with permission). Note that in these and other figures, the heat flows reported are based on the recorded sample weight, whereas for quantitative determination of properties such as the enthalpy of cure, the recorded sample weights are corrected using the enthalpy of fusion as an internal calibration standard (see Reference S3, Supporting Information, Section S6, for a discussion).

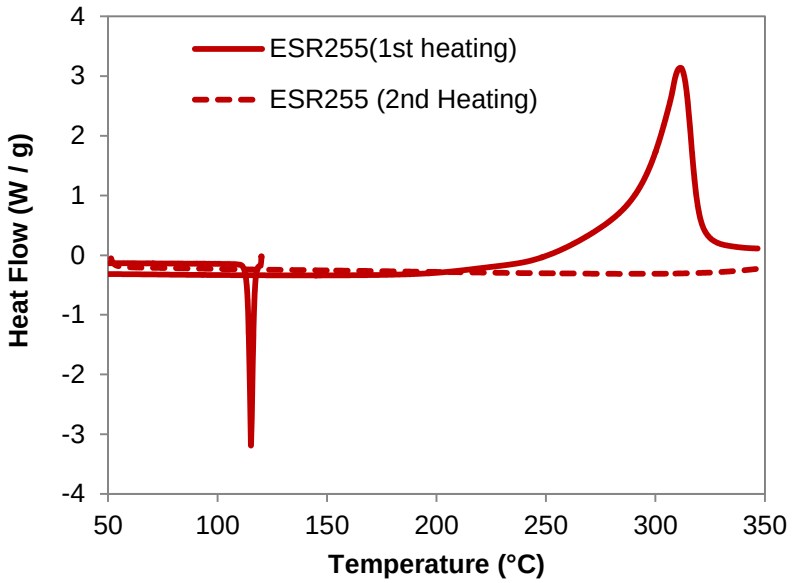

FIGURE S3. Non-isothermal DSC of ESR-255. Note in this case the first heating includes an initial rap to 120 °C to melt the sample, followed by cooling to -90 °C, and then re-heating of the supercooled sample through the cure protocol.

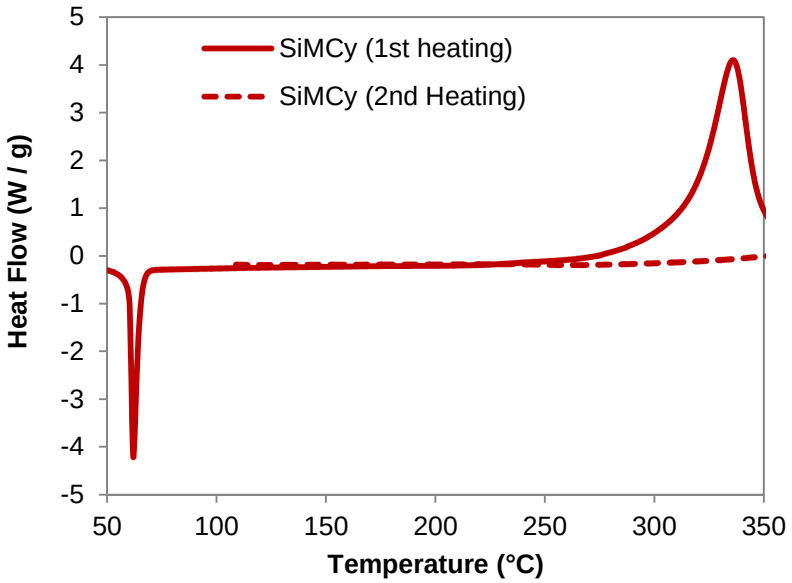

FIGURE S4. Non-isothermal DSC of SiMCy (further purified by flash chromatography)

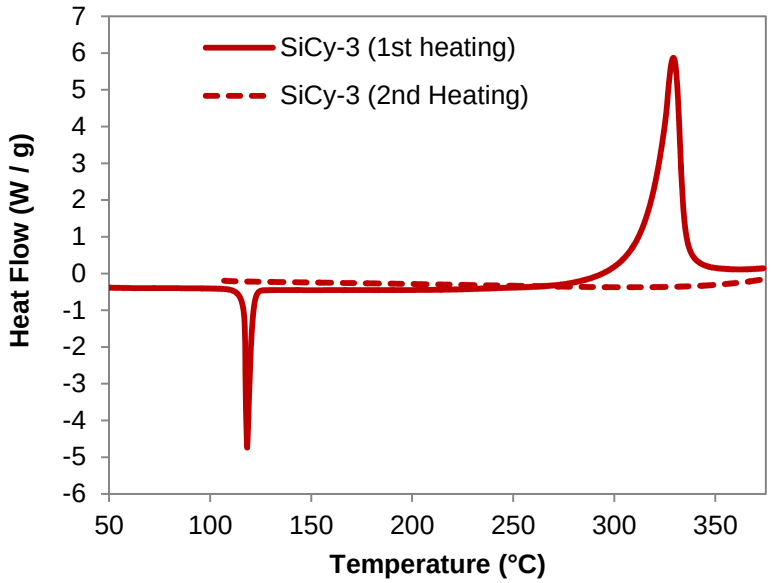

FIGURE S5. Non-isothermal DSC of SiCy-3 (batch 2, purified by flash chromatography). The maximum scan temperature was extended to 375 °C in order to capture the "L-shaped" exotherm that is characteristic of incomplete cure due to vitrification.[S3]

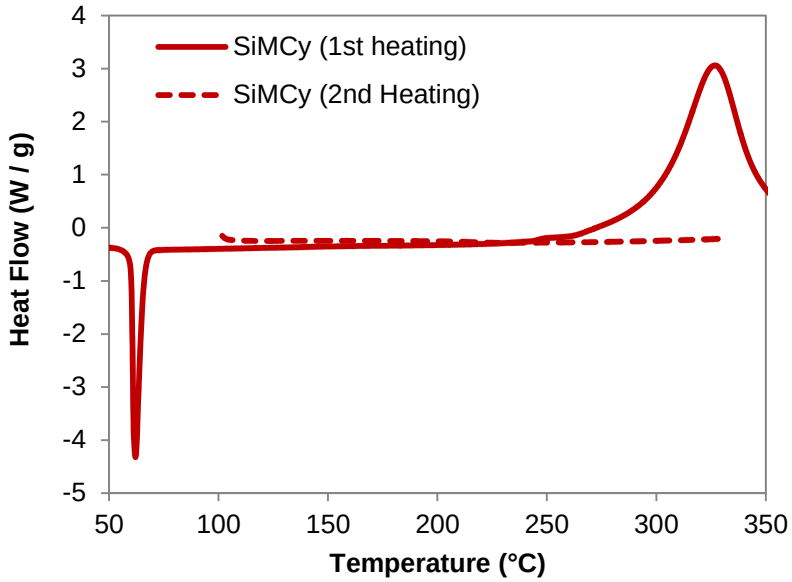

FIGURE S6. Non-isothermal DSC of SiMCy (as-synthesized)

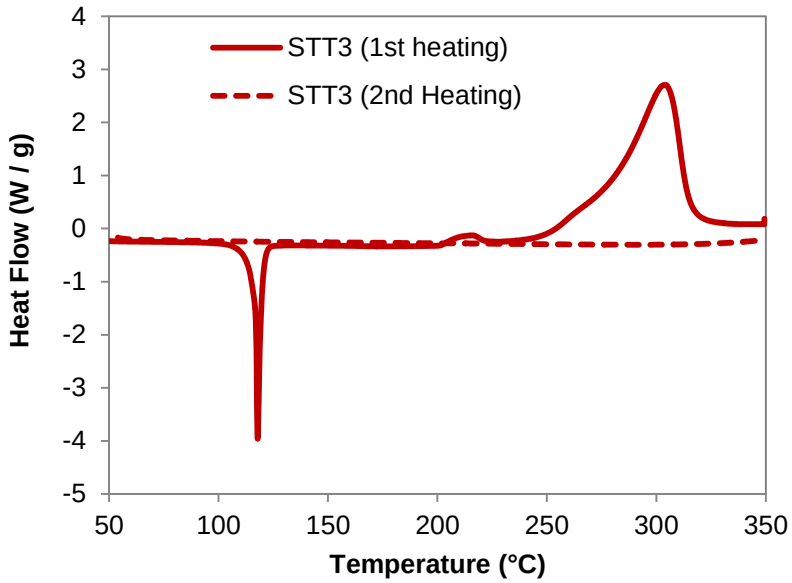

FIGURE S7. Non-isothermal DSC of SiCy-3 (as-synthesized)

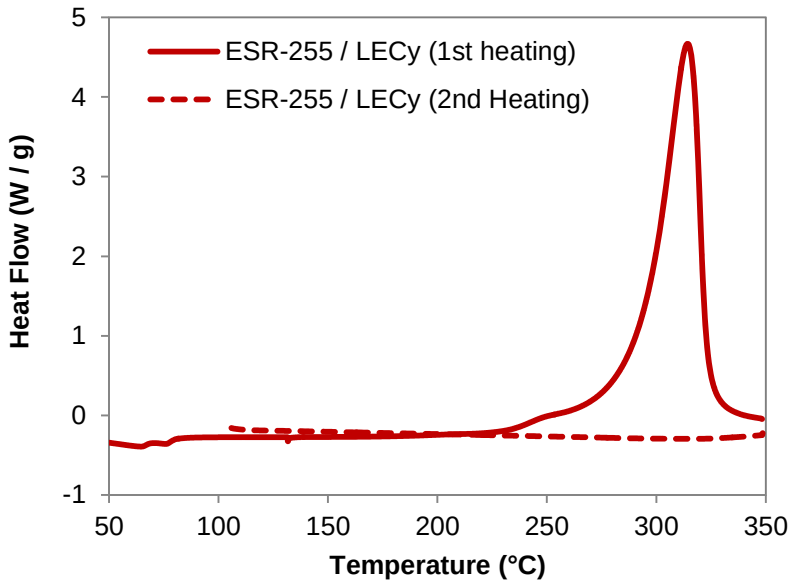

.

FIGURE S8. Non-isothermal DSC of a 50 / 50 (wt%) mixture of ESR-255 and Primaset® LECy

S3. Cure Kinetics / Isothermal DSC Data

TABLE S4 Comparative Kamal Model Cure Kinetics Analysis of Cyanate Ester Monomers

Monomer	Central Atom	*f*	Purification	*Temperature (°C)*	k_1' *(/s)*	k_2' *(/s)*	*m*	*n*
BADCy	C	2	As-Rec'd	270	0.00029	0.00043	1.75	1.13
BADCy	C	2	As-Rec'd	290	0.0026	0.022	1.83	1.46
SiMCy	Si	2	Chrom.	250	0.00025	0.0002	0.94	0.42
SiMCy	Si	2	Chrom.	270	0.00033	0.0018	1.25	0.85
SiMCy	Si	2	Chrom.	290	0.00076	0.0038	1.18	0.82
SiCy-3	Si	3	Chrom	270	0.00014	0.0049	1.54	1.19
SiCy-3	Si	3	Chrom	290	0.00025	0.011	1.39	1.21
SiCy-3 B2	Si	3	Chrom.	270	0.00019	0.0054	1.44	1.59
SiCy-3 B2	Si	3	Chrom.	290	0.00037	0.013	1.37	1.61
SiCy-3 B2 Run 2	Si	3	Chrom.	290	0.00042	0.013	1.61	1.66
SiMCy	Si	2	As Synth.	250	0.00023	0.0012	1.32	1.04
SiMCy	Si	2	As Synth.	270	0.00035	0.0025	1.13	0.95
SiMCy	Si	2	As Synth.	290	0.0011	0.0084	1.03	1.19

As-synthesized samples of SiCy-3 showed cure isotherms characteristic of catalyzed behavior, with no clear auto-catalytic maximum observed. Therefore, fitting of this data to the Kamal model was not attempted. Data for ESR-255 are available in Supporting Information of Reference S3. Note: only those runs showing achieving more than about 50% conversion, in which auto-catalytic behavior is clearly distinguishable, were fitted to individual Kamal model parameters. See Reference S3, Supporting Information, Section S6, for a complete description of the Kamal model parameters listed in this table.

TABLE S5 Comparative Kamal Model Cure Kinetics Analysis (Temperature-Independent Rate Constants) of Cyanate Ester Monomers

Monomer	Central Atom	f	Purification	*Temperature (°C)*	k_1 *(/s)*	k_2 *(/s)*	$\bar{m}$	$\bar{n}$
BADCy	C	2	As-Rec'd	210	0.000045	0.0008	1.788	1.291
BADCy	C	2	As-Rec'd	230	0.000055`	0.0010	1.788	1.291
BADCy	C	2	As-Rec'd	250	0.00026	0.0024	1.788	1.291
BADCy	C	2	As-Rec'd	270	0.00026	0.0052	1.788	1.291
BADCy	C	2	As-Rec'd	290	0.0026	0.019	1.788	1.291
SiMCy	Si	2	Chrom.	210	0.000021	0.00086	1.22	0.84
SiMCy	Si	2	Chrom.	230	0.00010	0.00023	1.22	0.84
SiMCy	Si	2	Chrom.	250	0.00026	0.00046	1.22	0.84
SiMCy	Si	2	Chrom.	270	0.00032	0.0018	1.22	0.84
SiMCy	Si	2	Chrom.	290	0.00078	0.0039	1.22	0.84
SiCy-3	Si	3	Chrom.	230	0.000029	0.00049	1.47	1.20
SiCy-3	Si	3	Chrom.	250	0.000043	0.0018	1.47	1.20
SiCy-3	Si	3	Chrom.	270	0.000086	0.0049	1.47	1.20
SiCy-3	Si	3	Chrom.	290	0.00031	0.012	1.47	1.20
SiCy-3 B2	Si	3	Chrom	230	0.000043	0.0021	1.47	1.62
SiCy-3 B2 Run 2	Si	3	Chrom	230	0.000039	0.00052	1.47	1.62
SiCy-3 B2	Si	3	Chrom	250	0.000046	0.0018	1.47	1.62
SiCy-3 B2	Si	3	Chrom	270	0.00017	0.0059	1.47	1.62
SiCy-3 B2	Si	3	Chrom	290	0.00045	0.014	1.47	1.62
SiCy-3 B2 Run 2	Si	3	Chrom	290	0.00020	0.013	1.47	1.62
SiMCy	Si	2	As-Synth.	210	0.000080	0.00032	1.08	1.07
SiMCy	Si	2	As-Synth.	230	0.00038	0.00077	1.08	1.07
SiMCy	Si	2	As-Synth.	250	0.00018	0.0011	1.08	1.07
SiMCy	Si	2	As-Synth.	270	0.00029	0.0028	1.08	1.07
SiMCy	Si	2	As-Synth.	290	0.0012	0.0078	1.08	1.07

As-synthesized samples of SiCy-3 showed cure isotherms characteristic of catalyzed behavior, with no clear auto-catalytic maximum observed. Therefore, fitting of this data to the Kamal model was not attempted. Data for ESR-255 are available in Supporting Information of Reference S3. See Reference S3, Supporting Information, Section S6, for a complete description of the Kamal model parameters listed in this table.

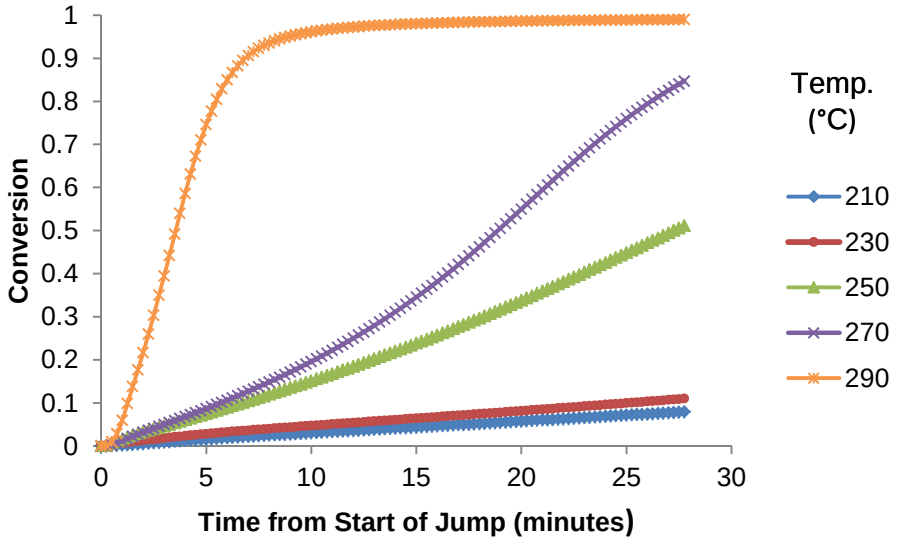

FIGURE S9 Isothermal cure kinetics of BADCy

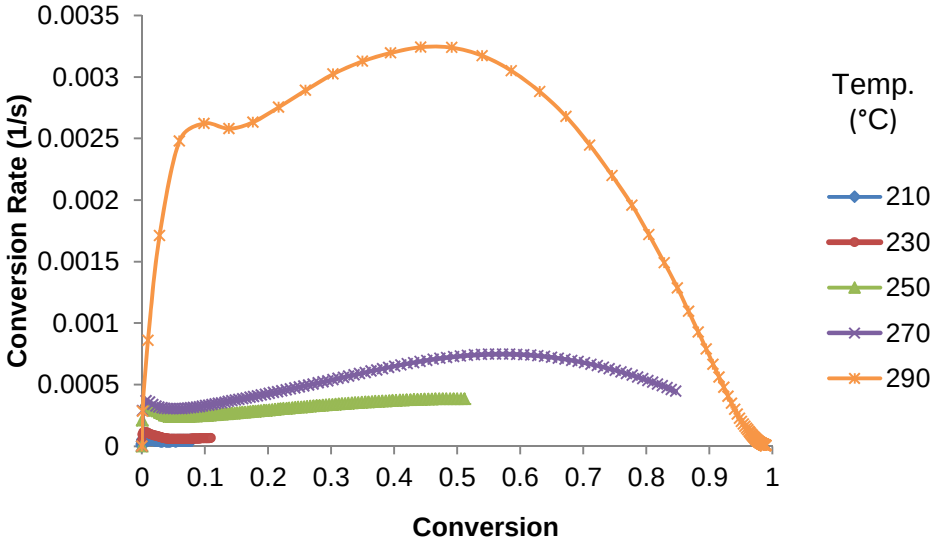

FIGURE S10 Conversion rate as a function of conversion during isothermal cure of BADCy

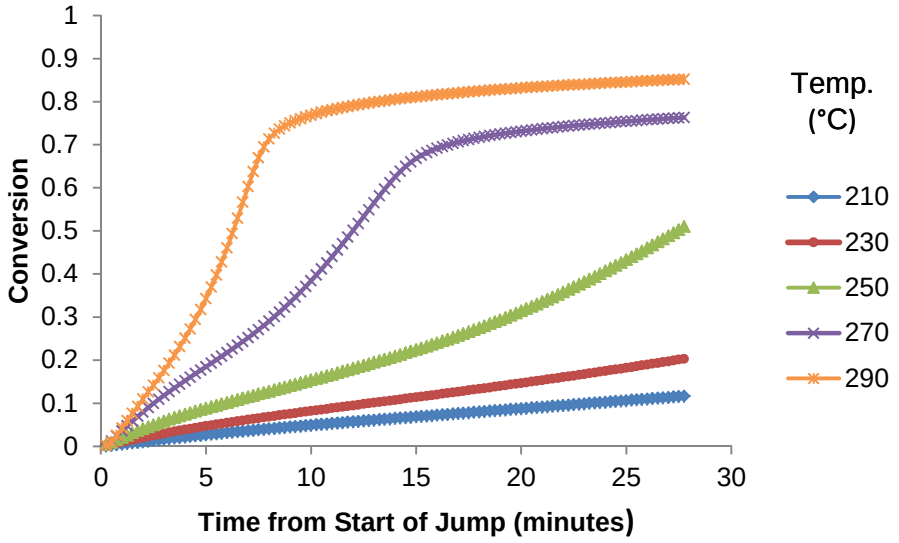

FIGURE S11 Isothermal cure kinetics of ESR-255 (reproduced with permission from Reference S3)

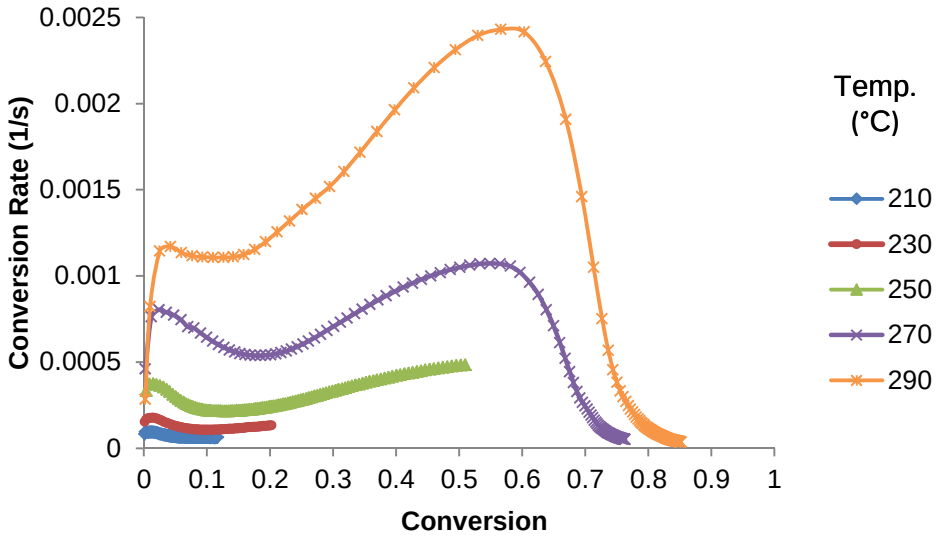

FIGURE S12 Conversion rate as a function of conversion during isothermal cure of ESR-255

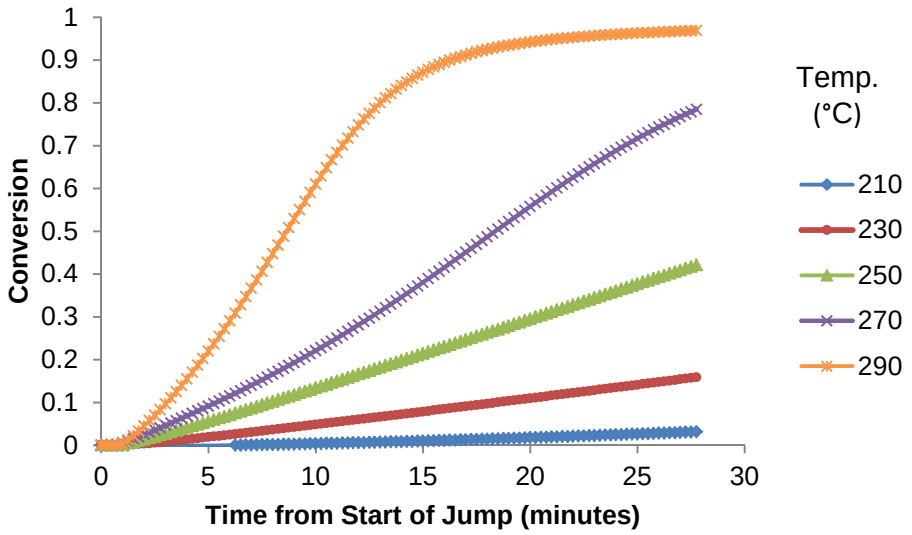

FIGURE S13 Isothermal cure kinetics of SiMCy (purified by flash chromatography)

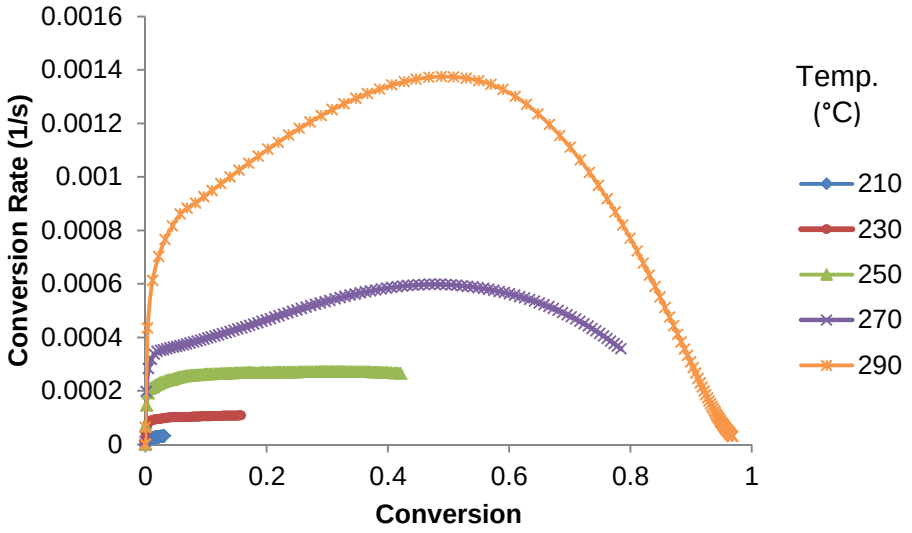

FIGURE S14 Conversion rate as a function of conversion during isothermal cure of SiMCy (purified by flash chromatography)

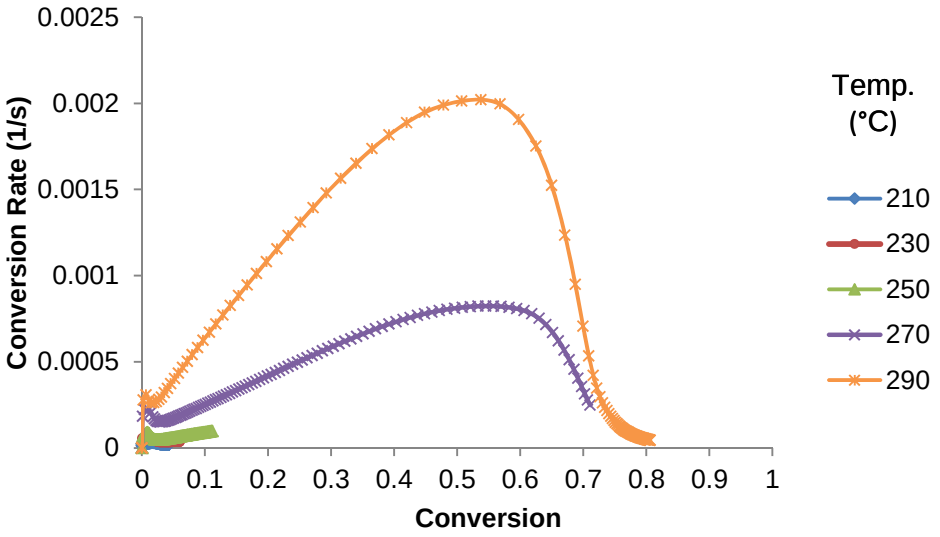

FIGURE S15 Conversion rate as a function of conversion during isothermal cure of SiCy-3 (purified by flash chromatography, batch 1). Conversion as a function of time for this sample is plotted in Figure 7 of the main manuscript.

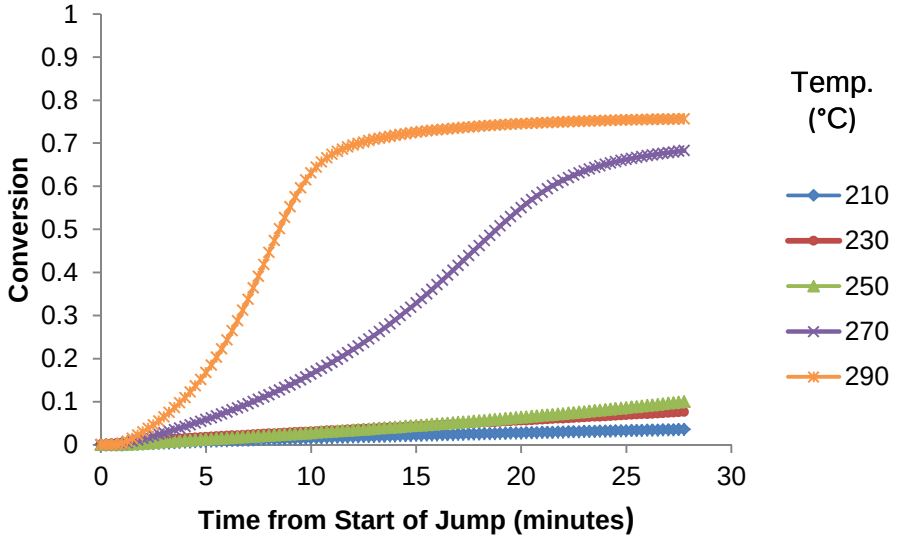

FIGURE S16. Isothermal cure kinetics of SiCy-3 (purified by flash chromatography, batch 2)

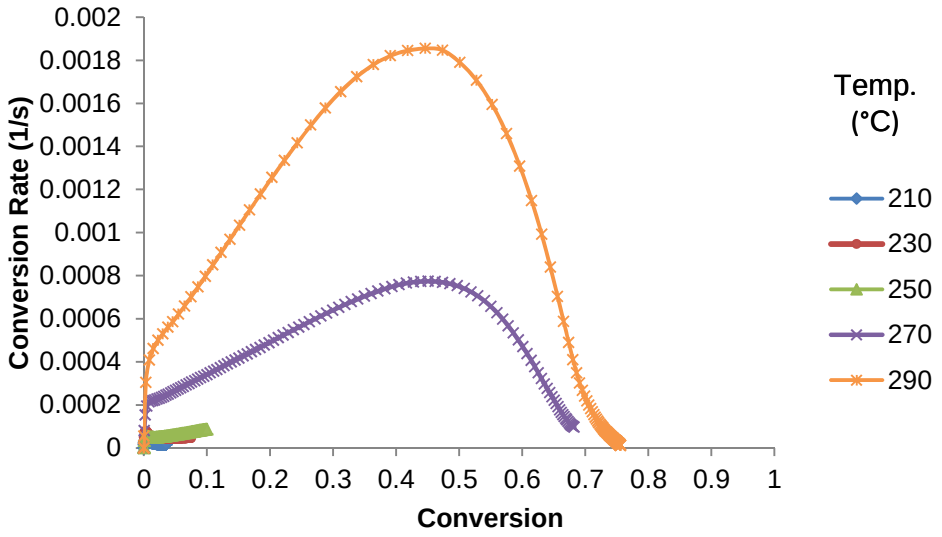

FIGURE S17 Conversion rate as a function of conversion during isothermal cure of SiCy-3 (purified by flash chromatography, batch 2).

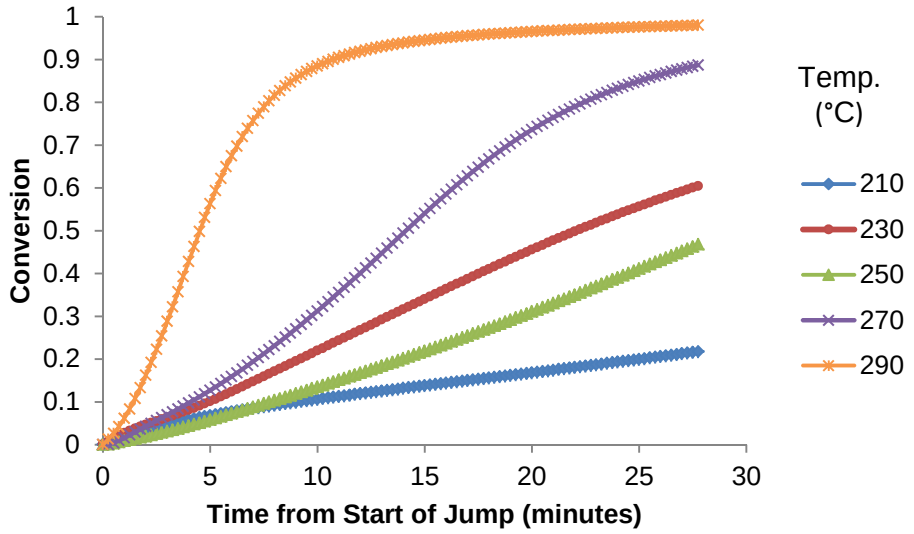

FIGURE S18 Isothermal cure kinetics of SiMCy (as-synthesized). Note that the rate of conversion for the 230 °C sample was unexpectedly high, but was reproducible (conversions after 30 minutes of 0.60 and 0.76 were obtained from the sample shown and its replicate). However, the effect disappeared upon further purification of SiMCy (see Figure S14).

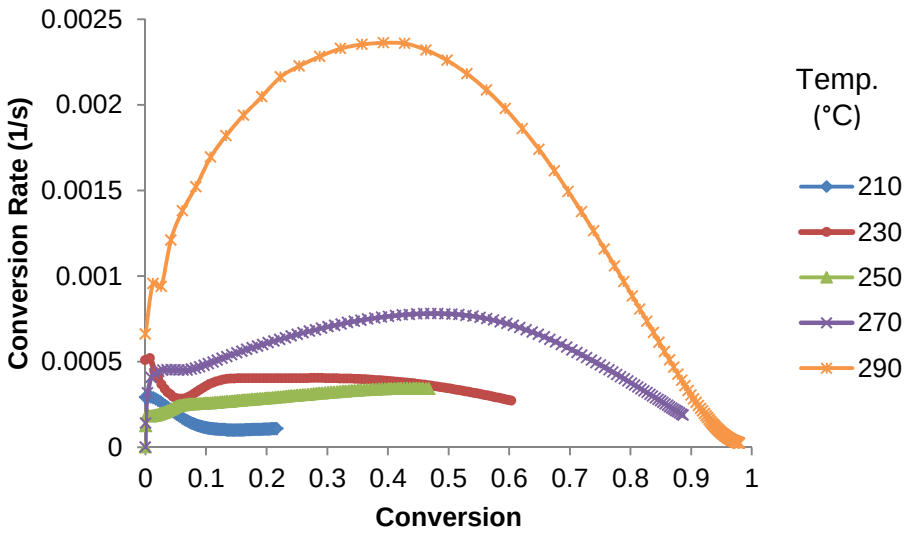

FIGURE S19 Conversion rate as a function of conversion during isothermal cure of SiMCy (as-synthesized). Note the unusually low conversion associated with the maximum conversion rate at 230 °C, an effect absent after further purification of SiMCy.

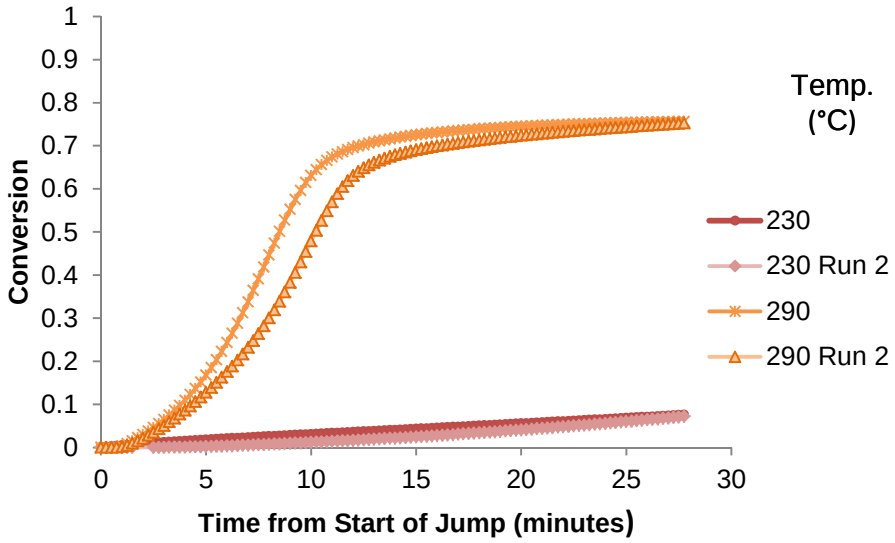

FIGURE S20 Reproducibility of isothermal kinetics data for SiCy-3 Batch 2 using selected temperature replicates.

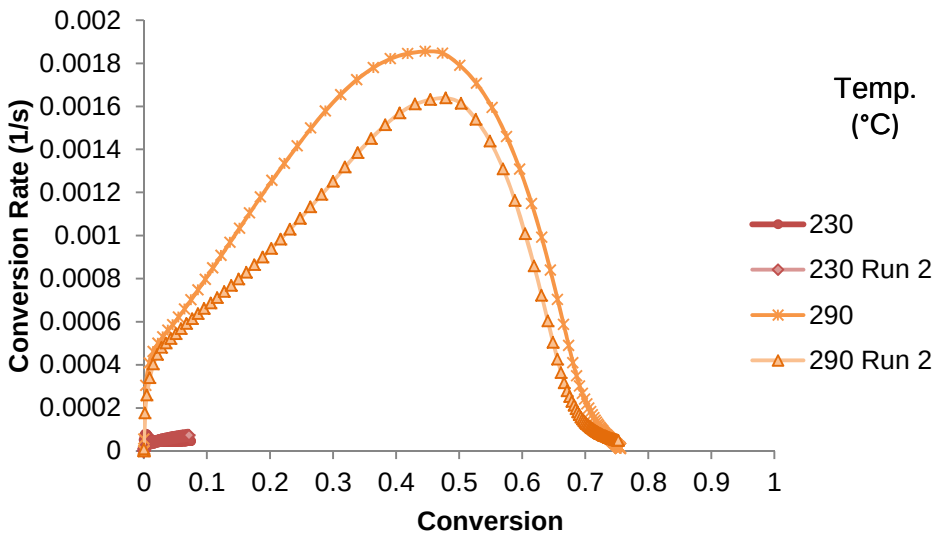

FIGURE S21. Reproducibility of conversion rate as a function of conversion for SiCy-3 Batch 2 using selected temperature replicates.

TABLE S6 Comparative Arrhenius Analysis of Cyanate Ester Monomer Reaction Kinetics and Miscellaneous Reaction Parameters

Monomer	Central Atom	*f*	Purification	$(d\alpha/dt)_{ac\text{-}max}$ *(/s) @250 °C*	E_a *(kJ/mol)*	*Temperature Ragne (°C)*	ΔH_{cure} [a] (kJ/eq.)
BADCy	C	2	As-Rec'd	0.00027 ± 0.00005	127 ± 20	250-290	113 ± 6
ESR-255	C	3	As-Rec'd	0.000385 ± 0.000005[b]	107± 1 [b]	250-290	105 ± 7[c,d]
SiMCy	Si	2	Chrom.	0.00012 ± 0.00003	131 ± 16	250-290	110 ± 5
SiCy-3	Si	3	Chrom.	0.000290 ± 0.000003	115 ± 1	250-290	n/a[d]
SiCy-3 B2[c]	Si	3	Chrom	0.00022 ± 0.00004	124 ± 8	250-290	n/a[d]
SiMCy	Si	2	As-Synth.	0.00024 ± 0.00001	120 ± 6	250-290	125 ± 3

[a] Based on isothermal cure at all temperatures studied and non-isothermal cure, regardless of whether the kinetic data was included in Arrhenius analysis. Note that full cure is not necessarily achieved by the isothermal and residual cure program, which features heating to 350 °C at 10 °C / min. [b] Data for ESR-255 is based on the kinetic parameters reported in Reference S3, re-analyzed to match the temperature range reported. [c] Reference S3 (Supporting Information) reports 830 J/g, or 105 kJ/eq., but rounds this to two significant figures to obtain 110 kJ/eq. with an uncertainty of 7 kJ/eq. [d.] Since full cure is not attained in these samples, only in the case of ESR-255, where DSC/IR studies have been performed as described in Reference S3, is the full enthalpy of cure estimated. The total enthalpy of cure as measured by DSC alone, which is the enthalpy released on heating to 350 °C, plus any enthalpy released during isothermal cure (if measurable with reasonable precision), from both isothermal and purely non-isothermal runs, is is 98 ± 3 kJ/eq. for ESR-255, 83 ± 8 kJ/eq. for SiCy-3 (Chrom., Batch 1), 88 ± 5 kJ/eq. for SiCy-3 (Chrom., Batch 2), 105 ± 4 kJ/eq. for SiCy-3 (As-Synth., uncorrected for 96% von t'Hoff purity),

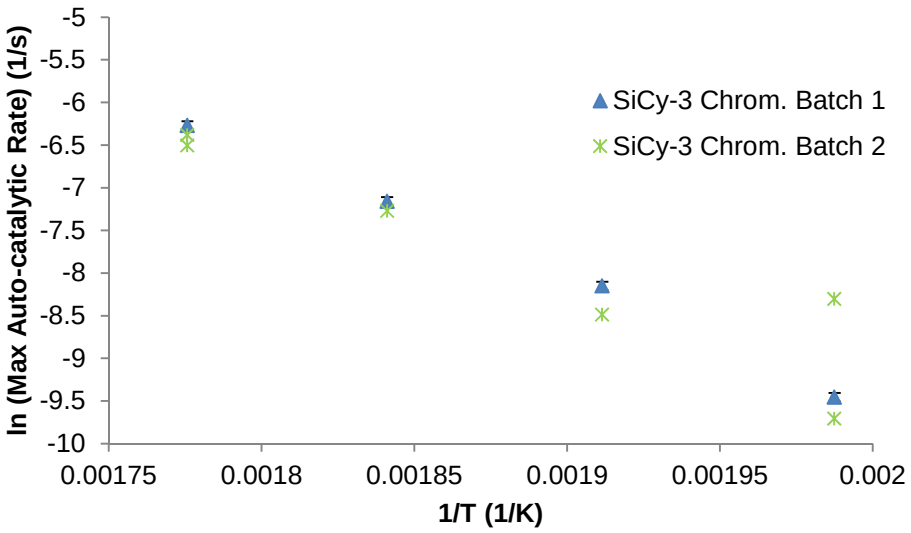

FIGURE S22 Arrhenius plot of two batches of highly purified SiCy-3. The maximum auto-catalytic rate, $(d\alpha/dt)_{ac\text{-}max} = k_2 \frac{\bar{m}^{\bar{m}}\bar{n}^{\bar{n}}}{(\bar{m}+\bar{n})^{(\bar{m}+\bar{n})}}$. This parameter is comparable across samples even when the kinetic parameters differ. In other words, while a higher value of k_2 for a particular sample does not necessarily indicate a characteristically faster reaction if $\bar{m}$ and $\bar{n}$ differ, a higher value of $(d\alpha/dt)_{ac\text{-}max}$ always indicates a characteristically faster reaction. Therefore, $(d\alpha/dt)_{ac\text{-}max}$ represents the best way to compare the reactivity of samples. The use of auto-catalytic, rather than total, reaction rates, helps to minimize the effect of impurities on the results. Characteristic reaction rates differ by about 10% both between batches, and between multiple samples within the same batch under the same conditions. The calculated activation energies for the two batches differ by about 7%. The analysis also shows that the data below 250 °C (right side of figure) is not highly repeatable, due to the low conversion rates at these temperatures.

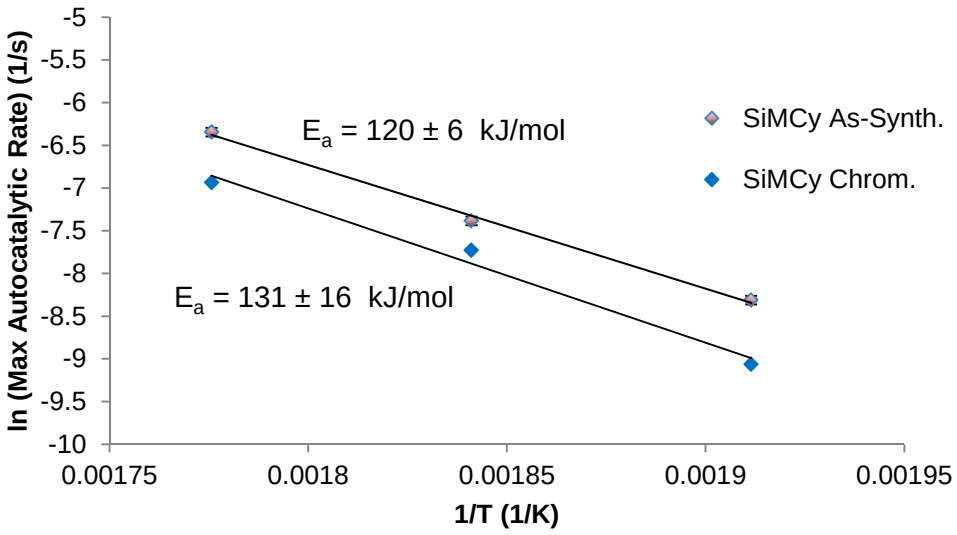

FIGURE S23 Arrhenius plot comparing SiMCy with von t'Hoff purities of 96% (as-synthesized) and >99% (purified via flash chromatography). The highly pure SiMCy reacts at about half the rate of the as-synthesized monomer, while the activation energies do not differ significantly.

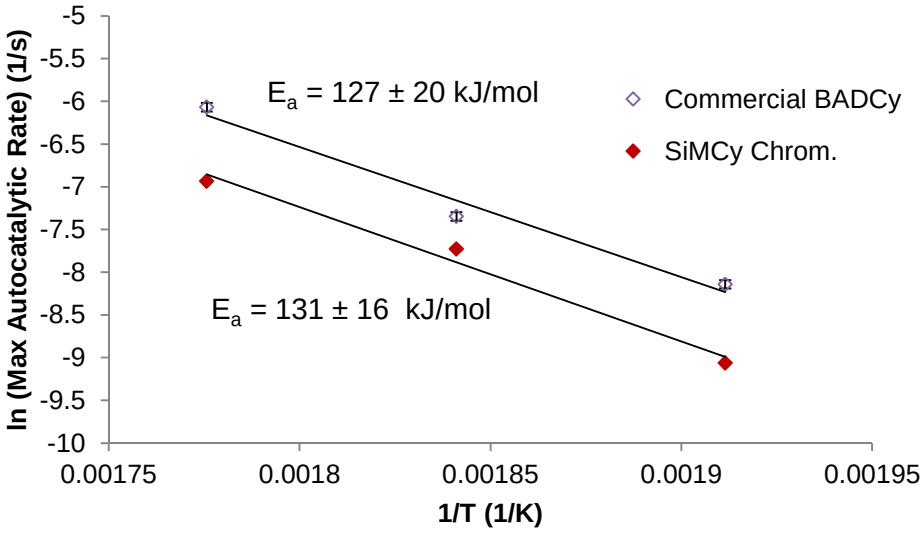

FIGURE S24 Arrhenius plot comparing BADCy and SiMCy. The activation energies are not significantly different.

S4. DSC Analysis of Cured Networks

TABLE S7 Comparative DSC Analysis of Cured Polycyanurate Networks

Monomer	Central Atom	*f*	Purification	Cure Condition (°C, hrs)[a]	T_G Signal Type[b]	T_G[c] (°C)	Conversion[d]	$T_{G\text{-full-cure}}$[e] (°C)
BADCy	C	2	As-Rec'd	None	Step	-38	0	305
BADCy	C	2	As-Rec'd	210, 0.5	n/a	n/a	0.08	301
BADCy	C	2	As-Rec'd	230, 0.5	n/a	n/a	0.10	300
BADCy	C	2	As-Rec'd	250, 0.5	n/a	n/a	0.51	309
BADCy	C	2	As-Rec'd	270, 0.5	Step	188	0.74	307
BADCy	C	2	As-Rec'd	290, 0.5	Step	308	0.99	313
BADCy	C	2	As-Rec'd	210, 12	Step	247	0.86[f]	311
ESR-255	C	3	As-Rec'd	210, 12	Onset	277 ± 1	0.75[g]	>340[h]
SiMCy	Si	2	Chrom.	None	n/a	n/a	0	250[i]
SiMCy	Si	2	Chrom.	210, 0.5	n/a	n/a	0.03	264
SiMCy	Si	2	Chrom.	230, 0.5	n/a	n/a	0.15	260
SiMCy	Si	2	Chrom.	250, 0.5	n/a	n/a	0.42	266
SiMCy	Si	2	Chrom.	270, 0.5	Step	188	0.78	273
SiMCy	Si	2	Chrom.	290, 0.5	Step	266	0.97	280
SiMCy	Si	2	Chrom.	210, 12	Step	214	0.88	274
SiCy-3	Si	3	Chrom.	None	Step	-6	0	>340[h]
SiCy-3	Si	3	Chrom.	210, 0.5	n/a	n/a	0.04	>340[h]
SiCy-3	Si	3	Chrom.	230, 0.5	n/a	n/a	0.06	>340[h]
SiCy-3	Si	3	Chrom.	250, 0.5	n/a	n/a	0.11	>340[h]
SiCy-3	Si	3	Chrom.	270, 0.5	Onset	277 ± 8	0.71	>340[h]
SiCy-3	Si	3	Chrom.	290, 0.5	Onset	315 ± 5	0.80	>340[h]
SiCy-3	Si	3	Chrom.	210,12	Onset	281 ± 2	0.62[g]	>340[h]
SiCy-3 B2	Si	3	Chrom.	None	n/a	n/a	0	>340[h]
SiCy-3 B2	Si	3	Chrom.	210, 0.5	n/a	n/a	0.03	>340[h]
SiCy-3 B2	Si	3	Chrom.	210, 0.5 Run 2	n/a	n/a	0.04	>340[h]
SiCy-3 B2	Si	3	Chrom.	230, 0.5	n/a	n/a	0.07	>340[h]
SiCy-3 B2	Si	3	Chrom.	230, 0.5 Run 2	n/a	n/a	0.08	>340[h]
SiCy-3 B2	Si	3	Chrom.	250, 0.5	n/a	n/a	0.10	>340[h]
SiCy-3 B2	Si	3	Chrom.	270, 0.5	Onset	283 ± 8	0.68	>340[h]
SiCy-3 B2	Si	3	Chrom.	290, 0.5	Onset	317 ± 3	0.75	>340[h]

SiCy-3 B2	Si	3	Chrom.	290, 0.5 Run 2	Onset	312 ± 14	0.75	>340[h]
SiMCy	Si	2	As-Synth.	None	n/a	n/a	0	216[i]
SiMCy	Si	2	As-Synth.	210, 0.5	n/a	n/a	0.22	251
SiMCy	Si	2	As-Synth.	230, 0.5	n/a	n/a	0.76	246
SiMCy	Si	2	As-Synth.	230, 0.5 Run 2	n/a	n/a	0.61	252
SiMCy	Si	2	As-Synth.	250, 0.5	n/a	n/a	0.47	251
SiMCy	Si	2	As-Synth.	270, 0.5	Step	196	0.87	251
SiMCy	Si	2	As-Synth.	290, 0.5	Step	252	0.98	245
SICy-3	Si	3	As-Synth.	None	Step	-7	0	>340[h]
SiCy-3	Si	3	As-Synth.	210, 0.5	n/a	n/a	0.42	>340[h]
SiCy-3	Si	3	As-Synth.	230, 0.5	Onset	242 ± 5	0.67	>340[h]
SiCy-3	Si	3	As-Synth.	250, 0.5	Onset	265 ± 9	0.81	>340[h]
SiCy-3	Si	3	As-Synth.	270, 0.5	Onset	297 ± 10	0.86	>340[h]
SiCy-3	Si	3	As-Synth.	290, 0.5	Onset	313 ± 9	0.87	>340[h]

[a] "Cure Condition" refers to the temperature and time used in the final cure step. For protocols with more than one step, the characteristics of the previous step are noted (all ramp rates were 5 °C unless otherwise noted. [b] T_G signal types: "step" means the standard step-change in heat capacity was visible; "onset" means that no such step change was visible. In such cases, if the apparent extent of cure (observed enthalpy during cure / (residual enthalpy + observed enthalpy)) was greater than 60%, the onset of residual cure was taken as the T_G. The validity of this approach has been shown previously.[S7] [c] Determined by residual enthalpy divided by total enthalpy in DSC scan for BADCy and SiMCy; determined by dividing residual enthalpy by 110 kJ/eq. for ESR-255 and SiCy-3 due to the inability to achieve full cure by heating to 350 °C. [d] T_G signal type for fully cured samples was always "step"; if no step change in heat capacity was visible, no value was reported.

S5. Thermo-mechanical Property Data

TABLE S8 Comparative Thermo-mechanical Property Data for Dry Cyanate Ester Monomers Cured at 210 °C for 24 hours

Monomer	Central Atom	*f*	Purification	Density (g/cc)	Coeff. Of Thermal Expansion (Fully Cured Network, @150 °C (ppm / °C)	T_G[a] from 1st TMA scan	T_G[b] "fully cured" from 2nd TMA scan
BADCy	C	2	As-Rec'd	1.208	n/a	275	323
ESR-255	C	3	As-Rec'd	1.270	n/a	245	>350[c]
SiCy-3 / LECy	Si	3 / 2	As-Synth.	1.226	58	>350[c]	>360[c]
SiCy-4 / LECy	Si	4 / 2	As-Synth.	1.258	50	340	>360[c]
SiCy-3	Si	3	As-Synth.	1.245	58	>350[c]	>360[c]
ESR-255 / LECy	C	3 / 2	As-Rec'd	1.256	n/a	323	>360[c]

[a] This value can be higher than the T_G at the completion of oven cure due to in-situ post-cure (see DSC data in Table S7 for a better estimate of T_G at the completion of oven cure), based on peak in loss component of dynamic stiffness [b] Value after heating to 350 °C, which may not reflect complete cure, based on peak in loss component of dynamic stiffness [c] No transition detected during scan, however values of stiffness indicate the same was in the glassy state throughout the scan

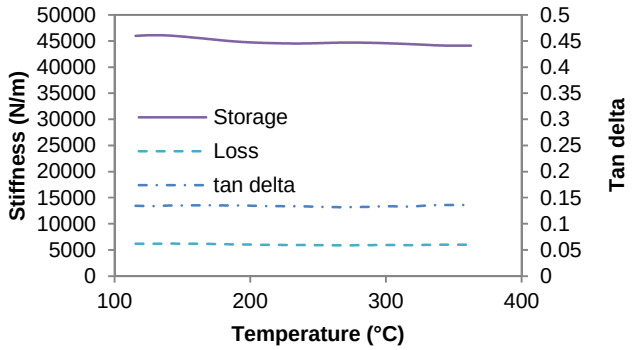

FIGURE S25 TMA of SiCy-3 (As-Synthesized) after heating to 350 °C (second scan, "fully cured")

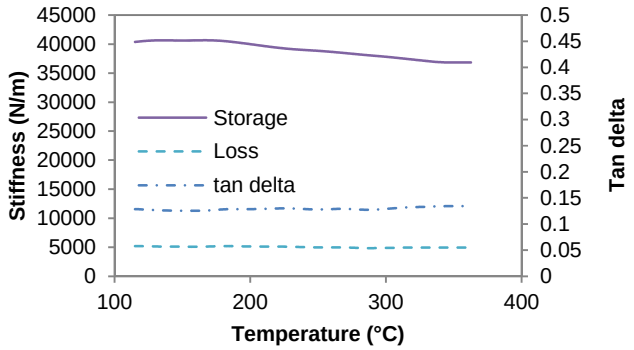

FIGURE S26 TMA of SiCy-3 (As-Synthesized) cocured with an equal weight of Primaset® LECy after heating to 350 °C (second scan, “fully cured”)

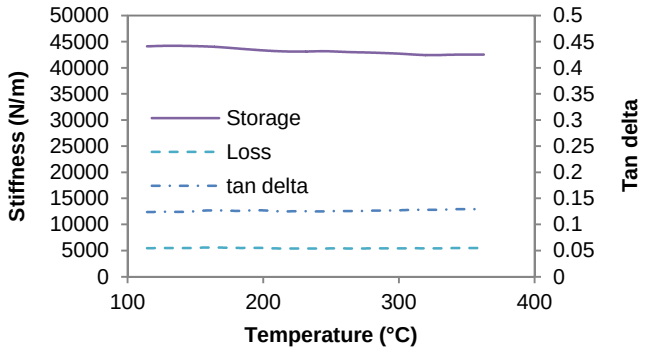

FIGURE S27 TMA of SiCy-4 (As-Synthesized) cocured with an equal weight of Primaset® LECy after heating to 350 °C (second scan, “fully cured”)

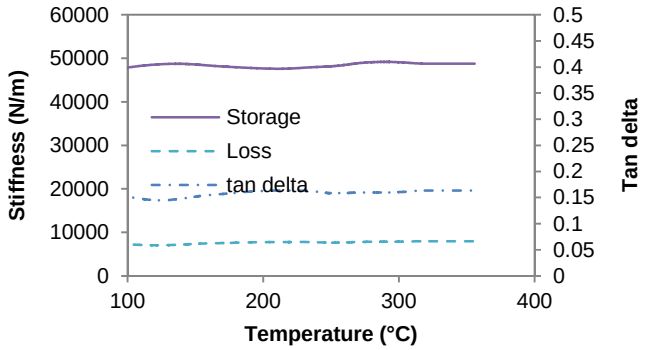

FIGURE S28 TMA of ESR-255 (As-Received) cocured with an equal weight of Primaset® LECy after heating to 350 °C (second scan, “fully cured”)

TABLE S9 Comparative Water Exposure (85 °C / 96 hr) Data for Cyanate Ester Monomers Cured at 210 °C for 24 hours

Monomer	Central Atom	*f*	Purification	Final Cure Temperature (°C)	Water Uptake (%)	T_G[a] after Exposure (°C)	T_G[a] “after Exposure and Heating to 350 °C (°C)
BADCy	C	2	As-Rec’d	210	1.34	240	Column 3
BADCy	C	2	As-Rec’d	250	2.75	n/a	n/a
ESR-255	C	3	As-Rec’d	210	3.54	224	Column 3
SiCy-3	Si	3	Chrom.	210	4.98	n/a	n/a
SiMCy	Si	2	As-Synth.	250	1.55	n/a	n/a

SiCy-3	Si	3	As-Synth.	210	5.54	202	225
SiCy-3 / LECy	Si	3 / 2	As-Synth.	210	4.37	226	208
SiCy-4 / LECy	Si	4 / 2	As-Synth.	210	4.73	247	244
ESR-255 / LECy	C	3 / 2	As-Rec'd	210	2.74	242	271

[a] Based on peak in loss component of dynamic stiffness

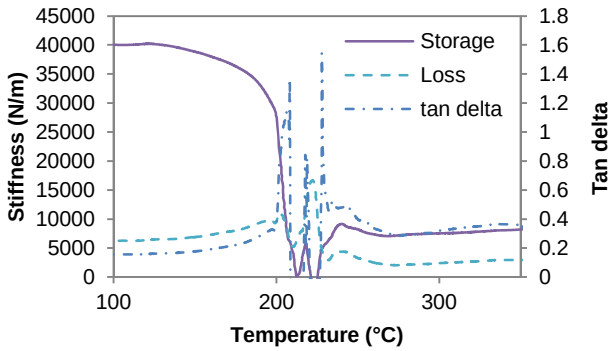

FIGURE S29 TMA of SiCy-3 (As-Synthesized) after cure for 24 hours at 210 °C followed by immersion in 85 °C water for 96 hours

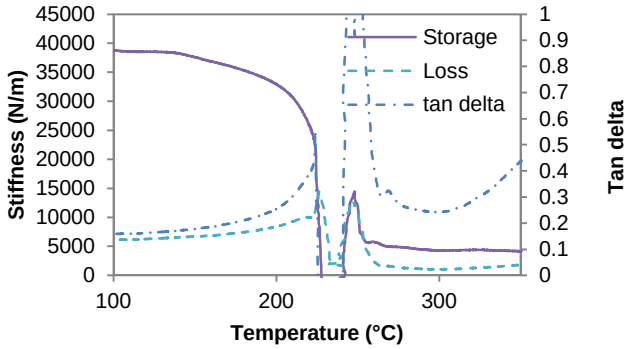

FIGURE S30 TMA of SiCy-3 (As-Synthesized) cocured with an equal weight of Primaset® LECy, after cure for 24 hours at 210 °C followed by immersion in 85 °C water for 96 hours

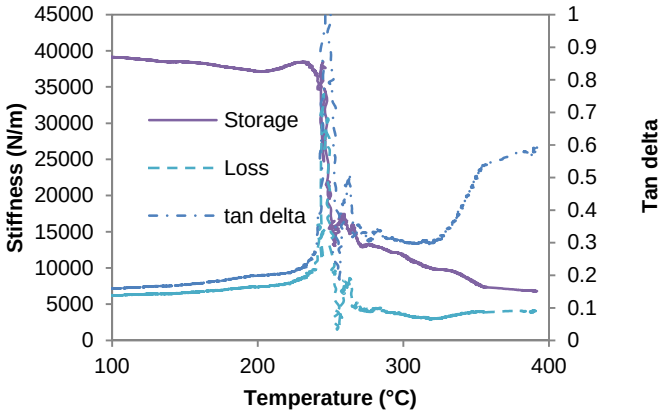

FIGURE S31 TMA of SiCy-4 (As-Synthesized) cocured with an equal weight of Primaset® LECy, after cure for 24 hours at 210 °C followed by immersion in 85 °C water for 96 hours.

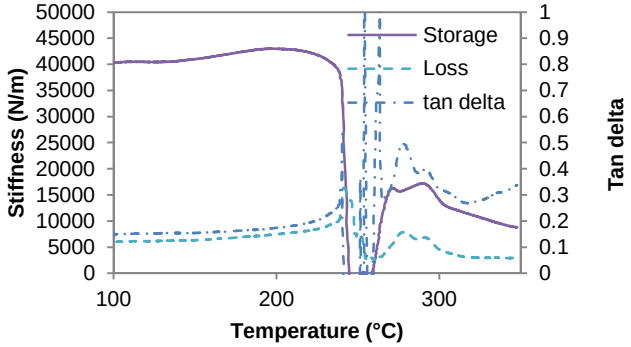

FIGURE S32 TMA of ESR-255 (As-Received) cocured with an equal weight of Primaset® LECy, after cure for 24 hours at 210 °C followed by immersion in 85 °C water for 96 hours.

S6. Thermogravimetric Analysis Data

TABLE S10 Comparative TGA Data for Cyanate Ester Monomers Cured at 210 °C for 24 hours

Monomer	Central Atom	*f*	Purification	T$_d$ 5% wt. Loss (in N_2, °C)	T$_d$ 5% wt. Loss (in air, °C)	Char Yield (in N_2, 600 °C)	Char Yield (in air, 600 °C)
BADCy	C	2	As-Rec'd	402	400	47%	25%
ESR-255	C	3	As-Rec'd	417	412	67%	59%
SiMCy	Si	2	As-Synth.	422[a]	409[a]	43%	50%
SiCy-3	Si	3	As-Synth.	405	400	55%	50%
SiCy-3 / LECy	Si	3 / 2	As-Synth.	402	396	63%	56%
SiCy-4 / LECy	Si	4 / 2	As-Synth.	409	395	70%	53%

ESR-255 / LECy	C	3 / 2	As-Rec'd	405	406	60%	2%

[a] Estimated from figures shown in Reference S6

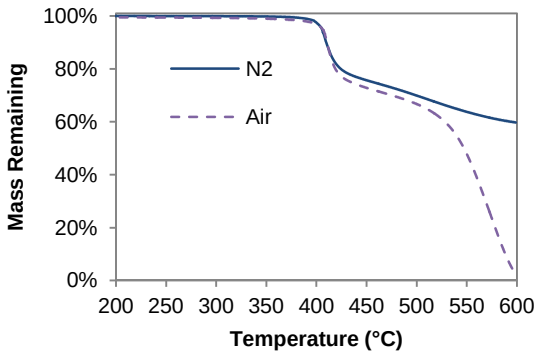

FIGURE S33 TGA traces (in nitrogen and air) of ESR-255 (As-Received) cocured with an equal weight of Primaset® LECy.

REFERENCES AND NOTES

S1. Davis, M. C.; Guenthner, A. J.; Groshens, T. J.; Reams, J. T.; Mabry, J. M. *J. Polym. Sci,. Part A: Polym. Chem.* **2012**, *50*, 4127-4136.

S2. Shimp, D. A.; Ising, S. J.; Christenson, J. R., Cyanate Esters -- A New Family of High Temperature Thermosetting Resins. In *High Temperature Polymers and Their Uses*, Society of Plastics Engineers: Cleveland, OH, 1989; pp 127-140.

S3. Guenthner, A. J.; Davis, M. C.; Ford, M. D.; Reams, J. T.; Groshens, T. J.; Baldwin, L. C.; Lubin, L. M.; Mabry, J. M. *Macromolecules* **2012**, *45*, 9707-9718.

S4. Guenthner, A. J.; Lamison, K. R.; Vij, V.; Reams, J. T.; Yandek, G. R.; Mabry, J. M. *Macromolecules* **2012**, *45*, 211-220.

S5. Reams, J. T.; Guenthner, A. J.; Lamison, K. R.; Vij, V.; Lubin, L. M.; Mabry, J. M. *ACS Appl. Matl. Interfaces* **2012**, *4*, 527-535.

S6. Guenthner, A. J.; Yandek, G. R.; Wright, M. E.; Petteys, B. J.; Quintana, R.; Connor, D.; Gilardi, R. D.; Marchant, D. *Macromolecules* **2006,** *39*, 6046-6053.

S7. Guenthner, A. J.; Reams, J. T.; Lamison, K. R.; Ramirez, S. M.; Swanson, D. D.; Yandek, G. R.; Sahagun, C. M.; Davis, M. C.; Mabry, J. M. *ACS Appl. Matl. Interfaces* **2013**, *5*, 8772-8783.